NASA TECHNICAL NOTE

NASA TN D-5926

EFFECTS OF THERMAL LOADING ON COMPOSITES WITH CONSTITUENTS OF DIFFERING THERMAL EXPANSION

by Charles A. Hoffman

Lewis Research Center
Cleveland, Ohio 44135

NATIONAL AERONAUTICS AND SPACE ADMINISTRATION • WASHINGTON, D. C. • AUGUST 1970

1. Report No. NASA TN D-5926	2. Government Accession No.	3. Recipient's Catalog No.
4. Title and Subtitle EFFECTS OF THERMAL LOADING ON COMPOSITES WITH CONSTITUENTS OF DIFFERING THERMAL EXPANSION		5. Report Date August 1970 6. Performing Organization Code
7. Author(s) Charles A. Hoffman		8. Performing Organization Report No. E-4768
9. Performing Organization Name and Address Lewis Research Center National Aeronautics and Space Administration Cleveland, Ohio 44135		10. Work Unit No. 129-03 11. Contract or Grant No.
12. Sponsoring Agency Name and Address National Aeronautics and Space Administration Washington, D.C. 20546		13. Type of Report and Period Covered Technical Note 14. Sponsoring Agency Code

15. Supplementary Notes

16. Abstract

Estimations have been made of elastic stresses and elastic-plastic stresses and strains which occur in laminate and in fiber composites. Calculated elastic tensile, compressive, and shear stresses for model tungsten-reinforced - 80Ni+20Cr-matrix laminate composites and fiber composites exceeded probable strengths of the respective constituents for a heat or cool cycle between 80° and 2000° F (26.5° and 1093.5° C). Elastic-plastic tensile and compressive stresses were less but calculated concurrent mechanical strain was sufficiently large to pose a thermal fatigue problem. Limited experimentation on tungsten-reinforced - 80Ni+20Cr-matrix laminate composites and on tungsten-reinforced - copper-matrix composites subjected to heat-cool cycles produced structural damage in most specimens in from 1 to 11 cycles. The minimum temperature was 80° F (26.5° C), and the maximum temperature was 2000° F (1093.5° C) for the laminate composite specimens and 1650° F (900° C) for the fiber composite specimens.

17. Key Words *(Suggested by Author(s))* Composite materials Thermal stresses	18. Distribution Statement Unclassified - unlimited

19. Security Classif. (of this report)	20. Security Classif. (of this page)	21. No. of Pages	22. Price*
Unclassified	Unclassified	80	$3.00

*For sale by the Clearinghouse for Federal Scientific and Technical Information
Springfield, Virginia 22151

CONTENTS

EFFECTS OF THERMAL LOADING ON COMPOSITES WITH CONSTITUENTS OF DIFFERING THERMAL EXPANSION

by Charles A. Hoffman

Lewis Research Center

SUMMARY

A heuristic study was conducted to analytically and experimentally evaluate the possible effects of differences in coefficients of thermal expansion of composite constituents on the structural integrity and performance of metal-metal composites. Both laminated sheet or foil and fiber types of composites were considered, and special reference was made to refractory-metal-reinforced superalloy matrix composites. Approximate equations were derived to permit the calculation of elastic stresses and elastic-plastic stresses and strains.

Stresses were calculated for model tungsten-reinforced - 80Ni+20Cr matrix composites of both laminate and fiber configuration. Heating and cooling between 80° and 2000° F (26.5° and 1093.5° C) was assumed. The elastic tensile, compressive, and peak shear stresses on heating or cooling could be far in excess of the tensile strengths and estimated shear strength. Approximate elastic-plastic analysis resulted in lowered stresses, but indicated concurrent strains of sufficient magnitude to cause thermal fatigue if heating and cooling cycles were encountered.

Limited experimental studies with tungsten-reinforced - 80Ni+20Cr-matrix laminate composites and slow heat-cool cycles between room temperature and 2000° F (1093.5° C) caused observable structural damage in 3 and 11 cycles for laminates with 0.020 and 0.005 inch (0.05 and 0.0125 cm) lamina, respectively; a 0.001-inch (0.0025-cm) lamina composite appeared undamaged at 11 cycles. Rapid heat-cool cycles produced observable damage in one, three, and six cycles for composites with 0.020-, 0.005-, and 0.001-inch (0.050-, 0.0125-, and 0.0250-cm) lamina, respectively. Six heat-cool cycles between room temperature and 1600° F (877° C) caused external change and microfracture of the matrix in a 0.70 volume fraction tungsten-fiber - copper-matrix composite; a 0.40 volume fraction tungsten-fiber composite sustained an external matrix crack after six such cycles. Heating the 0.70 volume fraction tungsten-fiber composite from room temperature to 1652° F (900° C) in a hot-stage microscope produced microfracture in the matrix. A 0.40 volume fraction tungsten-fiber composite exhibited severe matrix strain as a result of being heated from room temperature to 1652° F (900° C).

INTRODUCTION

There is, currently, considerable interest in composite materials: such materials offer many potential and demonstrated advantages for achieving higher use-temperatures and strength to weight ratios. Composites with superalloy matrices and refractory fiber reinforcements are being extensively studied in an effort to obtain materials for use at elevated temperatures (refs. 1 to 3). Some combinations of materials offer substantial promise for use in creep-rupture applications in the 2000° to 2200° F (1093.5° to 1205° C) range (ref. 2). Numerous other metal-fiber matrix composites, such as boron in aluminum, boron in titanium, boron in magnesium, silicon carbide in aluminum, silicon carbide in magnesium, and silicon carbide in titanium are also being considered, but for lower use-temperatures. Laminated sheet or foil composites have also received attention as a means of achieving more impact resistant or fracture resistant materials (refs. 4 to 6). Laminate composites can comprise alternating strong reinforcement laminae and ductile matrix laminae, bonded together. Laminated composites presumably can be relatively simply fabricated and may have less anisotropy than fiber-reinforced composites.

The successful use of dissimilar materials when used in composites, requires adequate compatibility between the materials. The complimentary aspects of a materials combination must outweigh any deleterious aspects. Many combinations of materials considered for use in reinforced metal-matrix composites have appreciable differences in the coefficients of thermal expansion of the reinforcement and the matrix. Typical superalloy matrices have coefficients of thermal expansion of about 9×10^{-6} to 10×10^{-6} inch per inch per $^{\circ}$F (16×10^{-6} to 19×10^{-6} m/(m)($^{\circ}$C)) over the temperature range of 80° to 2000° F (26.5° to 1093.5° C). The refractory metals that might be used for reinforcement (and presumably their alloys also) have coefficients of thermal expansion of about 3×10^{-6} inch per inch per $^{\circ}$F (54×10^{-6} m/(m)($^{\circ}$C)), over the same temperature range. The aluminum, titanium, and magnesium matrices can also have appreciable differences in their coefficients of thermal expansion compared with those of their reinforcements.

One would expect that thermal treatment (i.e., temperature cycling) given to materials having sufficient differences in thermal expansions could damage the composite by disrupting its structural integrity. Adverse effects could occur on cooling (or heating) the composite after initial consolidation treatment or during use when heating and cooling cycles are part of the exposure conditions.

This possible problem that could arise from the generation of residual thermal stresses has been recognized by others (e.g., refs. 3 and 7 to 9). Scala (ref. 7) calculated that elastic tensile stresses (i.e., 100 to 200 ksi (689 to 1380 MN/m^2)) far above matrix yield and ultimate tensile strengths could be developed in the matrices of some

composites. He also suggested that composites might fail as a result of shear stress along the bond interfaces. In reference 9, an analysis was made to determine the limiting coefficients of thermal expansion of possible metal reinforcing fibers incorporated into a ceramic matrix (e.g., ZrO_2). These limiting coefficients would then prevent matrix damage from occurring as a result of differential expansions due to assumed temperature changes.

The purpose of the present study was to gain a further understanding of the possible effects of differences in thermal expansions of metal-metal composite constituents on composite integrity and performance. This heuristic study has the following specific objectives:

(1) To develop approximate mathematical expressions for the internal stresses that might arise and to determine the approximate magnitudes of these stresses and their associated strains for a representative foil laminate composite and a representative fiber composite.

(2) To obtain experimental indication of the effect of thermal cycling and resultant thermal stress on composite integrity.

(3) To use the concepts gained from the analytical results and the experimental study results and to consider the practical significance of internal stresses and strains and ways of meliorating any possible adverse effects.

The scope of this study includes the derivation of approximate equations for elastic stresses that might be generated in laminate composites and in fiber composites because of thermal stresses arising from differences in coefficients of thermal expansion. The equations and auxiliary methods also permit the estimation of elastic-plastic stresses and strains. In addition, limited experimental studies are made on laminate and fiber composites to obtain practical indications of the possibility of composite damage from thermal stress-strain effects due to thermal expansion differences. The mathematical analysis is not intended to be rigorous at all times; such a rigorous treatment is beyond the scope of this report. Where existing derivations or methods of analysis were applicable, they were used in this study.

SYMBOLS

A total area

a area of fiber of sheet

b fiber radius

c radius of matrix associated with fiber (see appendix D)

D diameter of fiber (i.e., reinforcement) or associated matrix

E modulus of elasticity

G	shear modulus
K	ratio of transverse to longitudinal stresses (see appendix E)
ℓ	length of sheet or fiber
m	matrix breadth
N	number of elements (fibers or laminae)
P	total force or load
p	pressure
r	reinforcement breadth
T	temperature
t	thickness
u	matrix displacement
V	volume fraction
W	width of sheet
x	distance in x direction (see subscripts)
α	coefficient of linear thermal expansion
β	$(b/c)^2$
γ	shear angle
ϵ	mechanical strain
λ	parameter, see appendixes B and E
ν	Poisson's ratio
ρ	$(r/c)^2$
σ	tensile or compressive stress
τ	shear stress

Subscripts:

av	average
c	composite
E	elastic
e	equivalent
h	homogeneous
i	internal
m	matrix
o	external

p	plastic
R	radial direction
r	reinforcement
t	total mechanical strain
x, y, z	orthogonal directions
θ	tangential direction
1, 2	subscripts differentiating a given symbol

LAMINATE COMPOSITES

STRESSES IN LAMINATE COMPOSITES MADE FROM SHEET OR FOIL

Assumptions

The following assumptions are part of the analysis:

(1) Constituents are perfectly bonded to each other.

(2) Each constituent is homogeneous and isotropic, and each has the same Poisson's ratio.

(3) Tensile or compressive stresses are uniform through the thickness of each constituent.

(4) The loading is such that $\sigma_x = \sigma_y$; that is, a biaxial stress state exists in the laminae.

(5) Laminae thickness is assumed to be small compared with the other dimensions; therefore, σ_z is considered to be equal to zero.

(6) No interphase region exists.

Edge effects are not considered.

Mechanism of Stress Generation

The model is illustrated in figure 1. It is composed of two different sheet or foil materials, each with a different coefficient of thermal expansion. These two materials are alternately positioned and bonded together. It is assumed for this analysis that stress-free bonding has been accomplished at elevated temperature and that the composite is subsequently cooled down to room temperature. The same equation would be derived if stress-free bonding could be accomplished at room temperature and the compos-

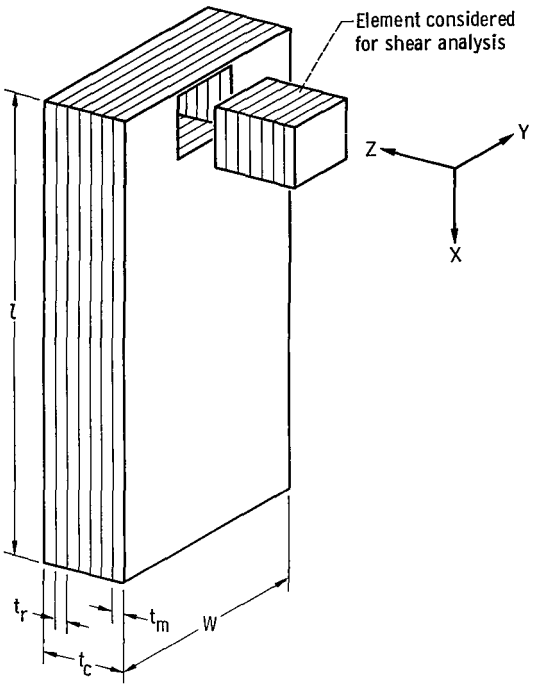

Figure 1. - Geometry of laminate composite showing alternating matrix and reinforcement laminae and element considered in the shear analysis.

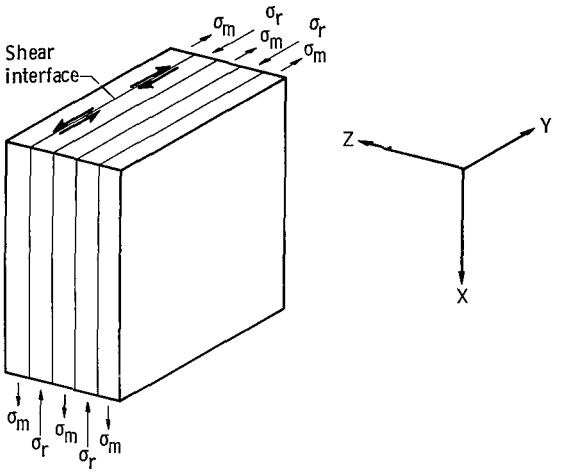

Figure 2. - Forces acting on element of laminate composite at some point away from ends; after cooling.

ite heated. It is apparent that, because of the bond between constituents, the constituent with the higher coefficient of thermal expansion will sustain a residual tensile stress (in the x and y directions) on cooling, and the constituent with the lower coefficient of thermal expansion will sustain a compressive stress (in the x and y directions) on cooling as indicated in figure 2. The reverse would be true if bonding took place, without stress, at room temperature and if the composite were then heated to an elevated temperature. The biaxial stress state (assumption (4)) will produce an equivalent stress. (Subsequent heating or cooling obviously would also produce stresses and strains, but not necessarily the same as those which occur on the initial thermal cycle; this because of possible changes in material properties or stress state.) The actual derivations are given in appendix A. The resultant equations for equivalent stress are

$$\sigma_{em} = \frac{V_r E_r E_m}{(V_r E_r + V_m E_m)(1 - \nu)} \left[(\alpha_r - \alpha_m)\Delta T + \frac{1}{2}(\epsilon_{erp} - \epsilon_{emp})\right] \tag{1}$$

$$\sigma_{er} = \frac{V_m E_m E_r}{(V_r E_r + V_m E_m)(1 - \nu)} \left[(\alpha_m - \alpha_r)\Delta T + \frac{1}{2}(\epsilon_{emp} - \epsilon_{erp})\right] \tag{2}$$

These equations may be used to calculate elastic and elastic-plastic stresses as well as elastic-plastic strains.

ELASTIC SHEAR STRESSES IN LAMINATE COMPOSITES

Assumptions

(1) Reinforcement and matrix are perfectly bonded to each other and are homogeneous, isotropic, and have the same Poisson's ratio.

(2) A state of equal biaxial stress exists (i.e., $\sigma_x = \sigma_y$).

(3) The stresses are in the elastic range.

(4) The stress σ_x is independent of y, away from edges.

(5) The thickness of the matrix is equal to or less than that of the reinforcement.

(6) No interphases exist.

Interacting edge effects are not considered (i.e., an element as shown in fig. 1 is considered).

Mechanism of Stress Generation

As a result of either heating or cooling a laminate composite after stress-free low- or high-temperature consolidation, shear stresses will be developed in the matrix of the composite since the matrix will expand or contract more than the reinforcement. The stresses developed by shear in the matrix after cooling and the strains developed as a result of matrix shear after cooling are illustrated in figures 3 and 4, respectively. These figures are discussed more fully in the derivation of the shear-stress equation in appendix B. The resultant equation for elastic shear stress is

$$\tau_{mzx} = \left[\frac{(\alpha_m - \alpha_r)\Delta T}{1 + \frac{(1 - \nu_m)}{(1 - \nu_r)} \left(\frac{E_r}{E_m}\right) \left(\frac{t_r}{t_m}\right)} \right] \frac{2G_m e^{-\lambda x/t_m}}{\lambda} \tag{3}$$

where

$$\lambda_1^2 = \left[\frac{4G_m(1 - \nu_r)t_m}{E_r t_r} \right] \tag{4}$$

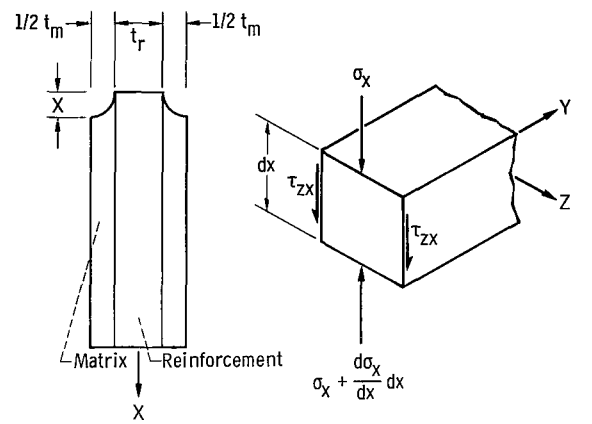

(a) Typical element. (b) Forces on reinforcement element.

Figure 3. - Element of laminate composite being considered and forces acting on the reinforcement after cooling.

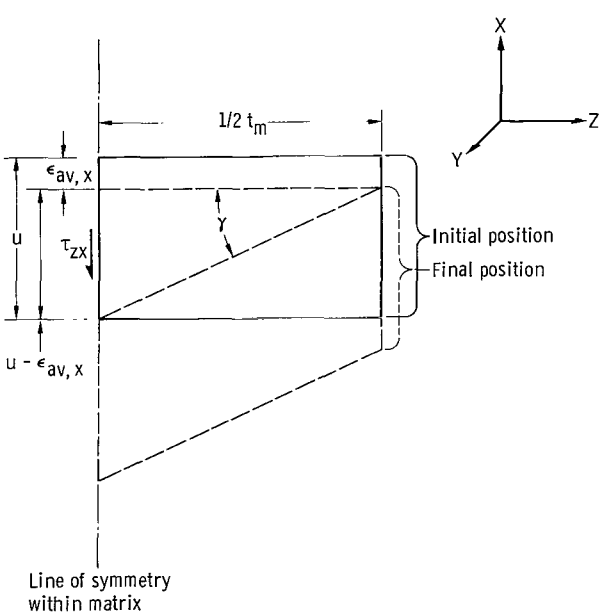

Figure 4. - One-half thickness of matrix element (side view, near tip) before cooling (initial position) and after cooling (final position).

CALCULATION OF RESIDUAL THERMAL STRESSES AND STRAINS IN MODEL SHEET OR FOIL LAMINATE COMPOSITES

Residual thermal stresses and strains have been calculated for sheet or foil reinforced laminate composites using equations (1) to (3). The calculations were made for two model specimens: one was assumed to have been consolidated at 2000° F (1093.5° C) (stress free) and then cooled to room temperature (condition A); the other consolidated in a stress-free manner at room temperature and heated to 2000° F (1093.5° C) (condition B). Condition A would also be analogous to a specimen exposed to 2000° F (1093.5° C) during use and cooled to room temperature; condition B would be analogous to a specimen being at room temperature and then exposed to 2000° F (1093.5° C). In both instances, the laminate composite specimens were assumed to be stress free at their respective initial temperatures. In these calculations the reinforcement is tungsten and the matrix is Nichrome V (80Ni+20Cr). The corresponding properties of importance are presented in table I.

The purpose of the calculations presented herein is to obtain indications of the magnitudes of thermally induced stresses and strains that might occur in use for tungsten reinforced 80Ni+20Cr. The calculated values of stresses and strains would be comparable to those in many other potential refractory-metal-reinforced - superalloy-matrix composites since the respective coefficients of linear thermal expansion are similar as are the moduli, Poisson's ratios, and yield strengths (see tables II to IV). The elevated temperature elastic modulus for the 80Ni+20Cr may be lower than that for other possible matrix materials so that those other materials could generate larger thermal stresses on heating.

TABLE I. - PROPERTIES OF CONSTITUENTS IN MODEL LAMINATE COMPOSITE

[Poisson's ratio is assumed to be 0.25 for both materials and at both temperatures.]

Material	Heating (80° F (26.5° C) to 2000° F (1093.5° C))				Cooling (2000° F (1093.5° C) to 80° F (26.5° C))			
	Modulus of elasticity, $E_{80^\circ F}$		Coefficient of linear thermal expansion, $\alpha_{80^\circ-2000^\circ F}$		Modulus of elasticity, $E_{2000^\circ F}$		Coefficient of linear thermal expansion, $\alpha_{80^\circ-2000^\circ F}$	
	psi	GN/m^2	in./in./°F	m/m/°C	psi	GN/m^2	in./in./°F	m/m/°C
Tungsten[a]	50×10^6	345	3×10^{-6}	5.4×10^{-6}	37×10^6	255	3×10^{-6}	5.4×10^{-6}
80Ni+20Cr[b]	30	307	[c]9.5	[c]17	[d]8	[d]56	[c]9.5	[c]17

[a]Based on data from ref. 10.
[b]Based on data from ref. 11.
[c]Based on data from ref. 12.
[d]Based on data from ref. 13.

TABLE II. - MEAN COEFFICIENT OF LINEAR THERMAL EXPANSION FOR SOME REFRACTORY AND SUPERALLOY MATERIALS

[All data obtained from ref. 13, unless otherwise noted.]

Material	Coefficient of linear thermal expansion, $\alpha_{80^{\circ}-2000^{\circ}F}$	
	in./in./$^{\circ}$F	m/m/$^{\circ}$C
Tungsten	3×10^{-6}	5.4×10^{-6}
Tantalum	3	5.4
Molybdenum	3.4	6.1
80Ni+20Cr[a]	9.5	17
René 41	10	18
Inconel 600	10	18
Hastelloy X	9.5	17
Nimonic 80[b]	10	18
GMR 235	9.8	17.2
Nichrotung	9.5	17
L-605	10	18
S-816	9.2	16.6
Wi-52	9.8	17.2
Mar M302	9.0	16.2

[a]Data from ref. 12.

[b]For room temperature to 1600° F (877° C).

TABLE III. - YIELD AND TENSILE STRENGTHS FOR SOME BULK REFRACTORY AND SUPERALLOY MATERIALS

[All data were based on ref. 13 unless otherwise noted.]

Materials	Temperature, °F (°C)							
	80 (26.5)				2000 (1093.5)			
	Strength							
	Yield		Ultimate tensile		Yield		Ultimate tensile	
	ksi	MN/m^2	ksi	MN/m^2	ksi	MN/m^2	ksi	MN/m^2
Tungsten	---	---	160	1110	---	---	60	414
Tantalum	70	484	155	1070	10	69	20	138
Molybdenum	100	689	170	1170	40	267	80	551
80Ni+20Cr	[a]70	484	[a]117	[a]807	5	35	5	55
René 41	40	276	180	1240	30	207	70	484
Inconel 600	35	242	124	900	5	35	8	55
Hastelloy X	60	415	110	780	---	---	30	207
Nimonic 80	90	624	155	1070	5	35	5	35
GMR 235	95	656	155	1070	35	242	80	551
Nichrotung	120	830	130	898	22	152	25	173
L-605	80	551	160	1100	35	245	40	276
S-816	80	551	140	918	---	---	10	69
WI-52	65	449	90	624	18	125	20	138
Mar M302	90	624	140	968	20	138	20	138

[a]Based on data from ref. 11.

TABLE IV. - ELASTIC MODULI FOR SOME REFRACTORY AND SUPERALLOY MATERIALS

[All data based on ref. 13.]

Material	Temperature, °F (°C)				Material	Temperature, °F (°C)			
	80 (26.5)		2000 (1093.5)			80 (26.5)		2000 (1093.5)	
	Elastic moduli, E					Elastic moduli, E			
	ksi	MN/m^2	ksi	MN/m^2		ksi	MN/m^2	ksi	MN/m^2
Tungsten	50	345	37	255	Hastelloy	30	207	16	110
Tantalum	28	193	25	173	Nimonic 80	27	186	7	48
Molybdenum	45	311	28	193	GMR 235	30	207	18	124
80Ni+20Cr	[a]30	207	8	55	Nichrotung	[b]34	235	[b]22	152
René 41	32	221	16	110	L-605	34	235	20	138
Inconel 600	30	207	8	55	S-816	35.5	245	24	166

[a]Based on data from ref. 11.
[b]Dynamic modulus.

Tensile and Compressive Stresses on Assumption of Elastic Strain

Cooling. - Thermally induced equivalent elastic stresses[1] are presented in figure 5(a) for a stress-free specimen having been cooled from 2000° F (1093.5° C) to 80° F (26.5° C) and in figure 5(b) for a stress-free specimen at 80° F (26.5° C) having been heated to 2000° F (1093.5° C). In figure 5(a), it is seen that matrix tensile stresses as high as approximately 550 ksi (3790 MN/m^2) can be developed in a high volume-fraction reinforcement composite and that reinforcement compressive stresses as high as about 900 ksi (6200 MN/m^2) can be generated in a high volume-fraction matrix composite. Tensile and compressive stresses of such high magnitudes could not be achieved because

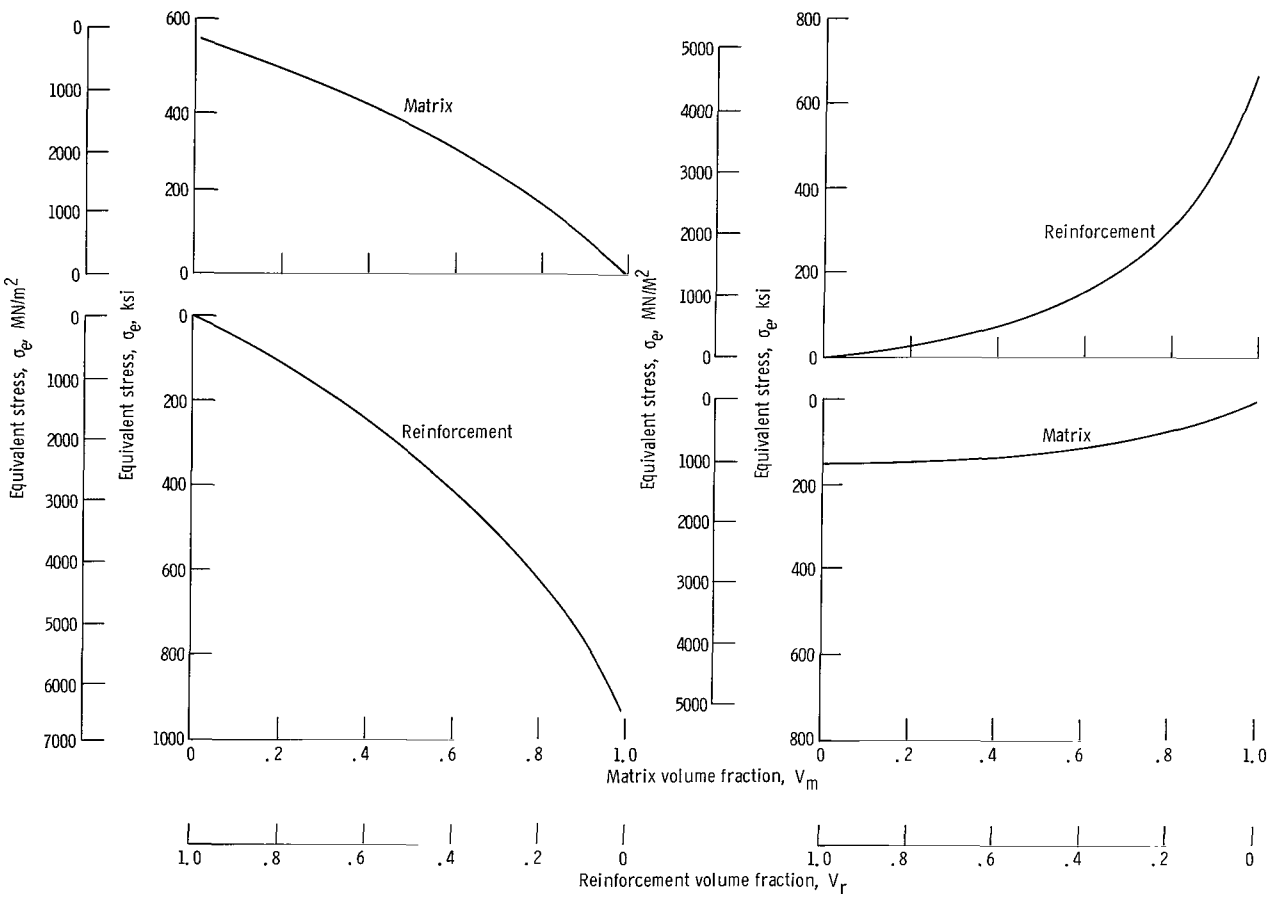

(a) Cooled from 2000° to 800° F (1093° to 26.5° C). (b) Heated from 80° to 2000° F.

Figure 5. - Equivalent elastic stress calculated for model tungsten - 80Ni+20Cr composite.

[1]The values of stress and strain must obviously become zero when the volume fraction of either constituent is zero; that is, the equations are valid only over the interval $0 < V_{m,r} < 1$ and must be zero at these limits.

they can far exceed both the yield and ultimate tensile strengths of the constituents. Yielding or fracturing of either constituent would be expected when its stress became sufficiently high.

Heating. - Upon heating from 80° F (26.5° C) to 2000° F (1093.5° C), equivalent elastic matrix compressive stresses as high as about 150 ksi (1030 MN/m^2) could be generated for a high volume-fraction reinforcement composite and equivalent elastic reinforcement tensile stresses as high as about 700 ksi (4820 MN/m^2) will be generated in a low volume-fraction reinforcement composite. Again, in either instance, yielding or fracturing could occur in the constituent whose yield or ultimate strength has been exceeded.

Tensile and Compressive Stresses and Strains on Assumption of Elastic-Plastic Deformation

The method and assumptions used in obtaining these values are discussed in appendix A.

Cooling. - Thermally induced equivalent elastic-plastic stresses are presented in figure 6(a) for specimens having been cooled from 2000° F (1093.5° C) and in figure 6(b)

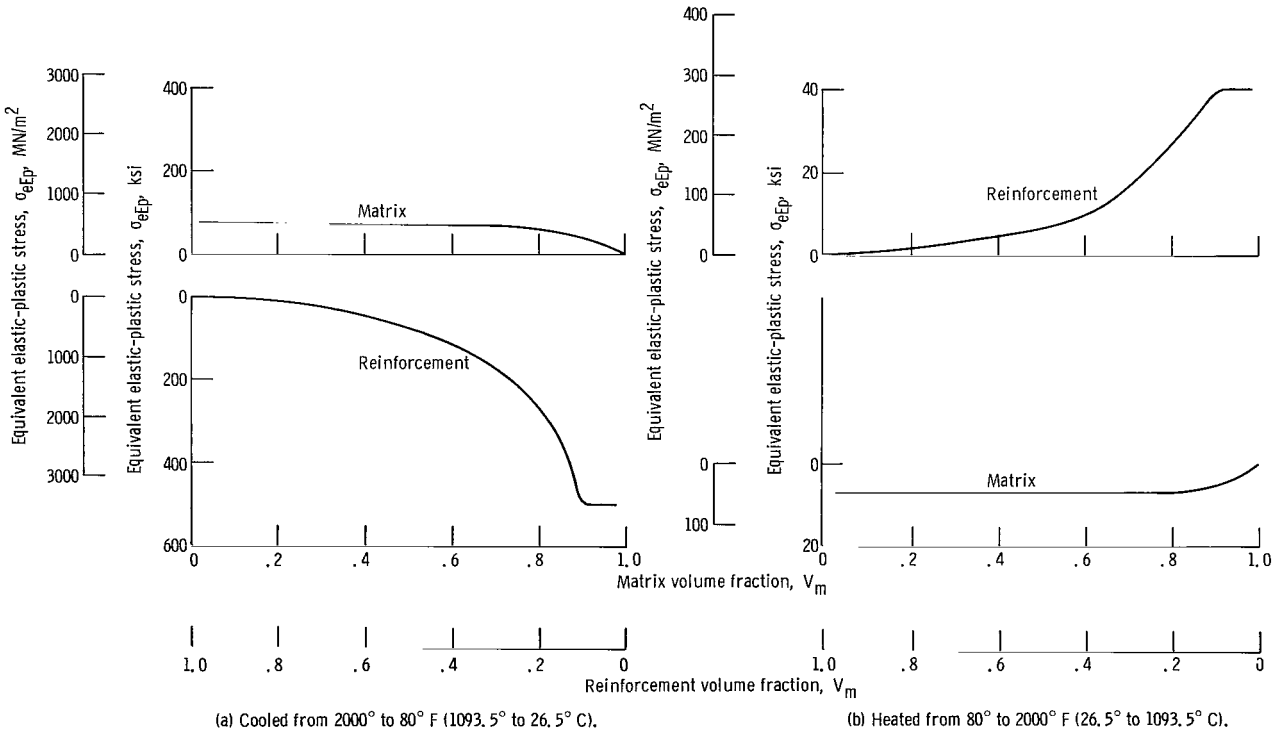

(a) Cooled from 2000° to 80° F (1093.5° to 26.5° C).

(b) Heated from 80° to 2000° F (26.5° to 1093.5° C).

Figure 6. - Equivalent elastic-plastic stress calculated for model tungsten - 80Ni+20Cr composite.

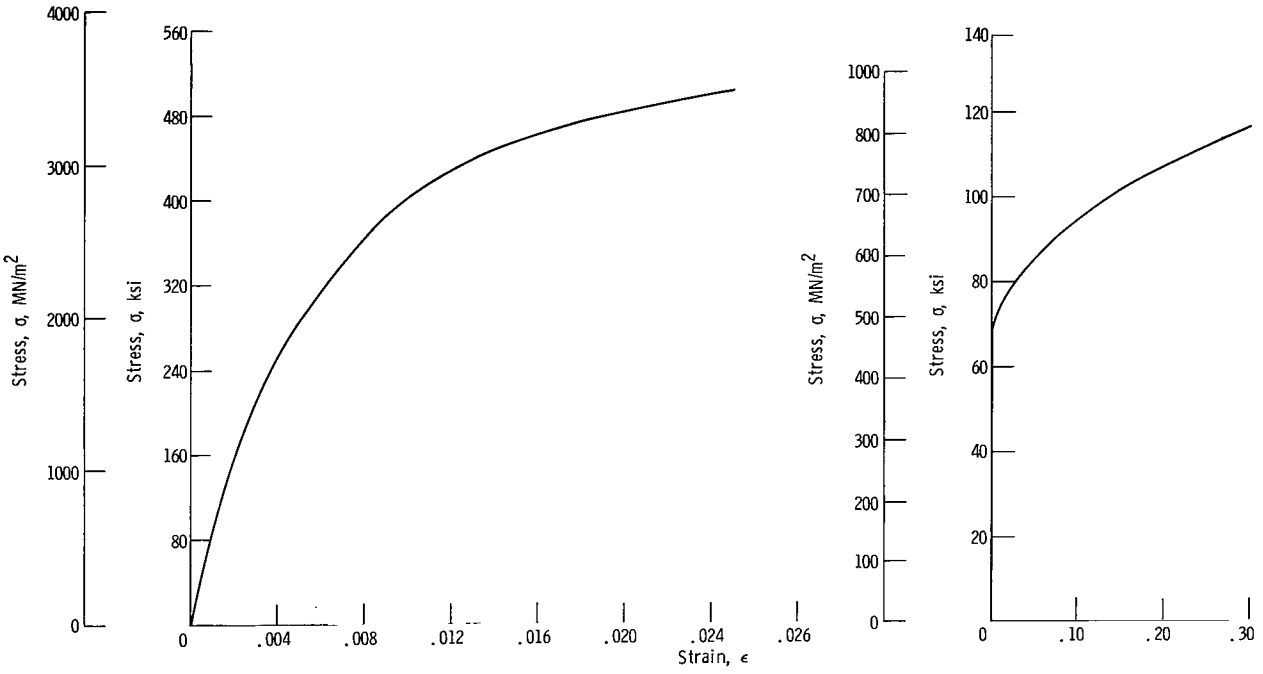

(a) Tungsten at room temperature (ref. 10).

(b) 80Ni + 20Cr at room temperature (ref. 11).

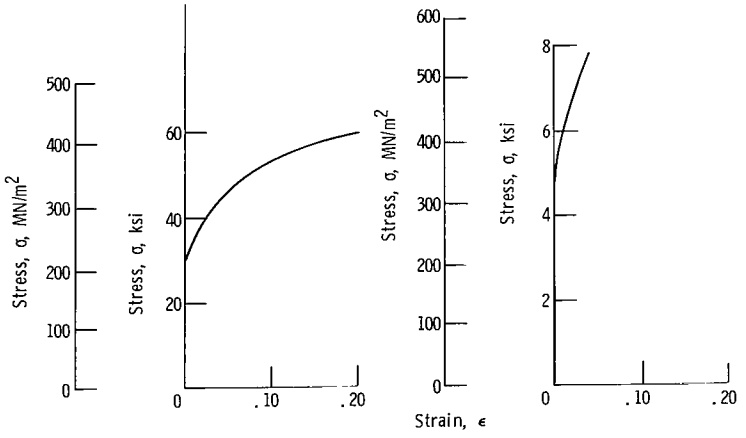

(c) Tungsten at 2000° F (1093.5° C) (ref. 10).

(d) 80Ni+20Cr at 2000° F (1093° C) (ref. 13).

Figure 7. - Uniaxial stress as function of strain.

for specimens having been heated to 2000° F (1093.5° C). The values shown in these curves were obtained using a graphical procedure described in appendix A and using the stress-strain diagrams of figures 7(a) and (b), which are based on references 10 and 11. (A sample calculation is shown in table V.) In either instance, the stresses, for given relative amounts of reinforcement, are less than the calculated elastic stresses. Upon cooling, the maximum matrix tensile stress can be as high as about 76 ksi (524 MN/m^2), and the maximum reinforcement compressive stress can be as high or about 500 ksi (3440 MN/m^2) for high volume-fraction reinforcement and high volume-fraction matrix composites, respectively.

TABLE V. - SAMPLE CALCULATION OF ELASTIC-PLASTIC STRESS AND STRAIN FOR TUNGSTEN - 80Ni+20Cr COMPOSITE

[Stresses and strains due to cooling from 2000° F (1093.5° C) to 80° F (26.5° C); matrix volume fraction, 0.1; reinforcement volume fraction, 0.9; equivalent reinforcement plastic strain, ϵ_{erp} is nil for this example.]

Equivalent matrix stress				Equivalent matrix plastic strain, ϵ_{emp}	Equivalent reinforcement stress				Total equivalent plastic strain, ϵ_{ept}
σ_{em}		$0.1\ \sigma_{em}$			σ_{er}		$0.9\ \sigma_{er}$		
ksi	MN/m^2	ksi	MN/m^2		ksi	MN/m^2	ksi	MN/m^2	
110	758	11	78	0.22	-12	-83	-11	-7.8	0.22
100	689	10	60	.14	-10	-69	-9.9	-6.9	.14
90	624	9	62	.08	-9.9	-69	-9	-6.2	.08
80	551	8	55	.04	-8.8	-61	-8	-5.5	.04
[a]78.5	541	7.85	54	.0250	-8.7	-60	-7.85	-5.4	.025
70	482	7	48	.002	-7.7	-53	-7	-4.8	.002

[a]Value where $P_{em} + P_{er} = 0$ and $\epsilon_{emp} - \epsilon_{erp} = 0.025 = \epsilon_{cpt}$.

Heating. - Upon heating stress-free specimens from room temperature, the maximum matrix equivalent compressive stress is about 7 ksi (48 MN/m^2) for high volume-fraction reinforcement composites, and the maximum reinforcement equivalent tensile stress is about 40 ksi (276 MN/m^2) for high volume-fraction matrix composites. The stresses generated by cooling or heating would not be expected to cause failure of either constituent. However, when heating and cooling cycles are applied, the effect could be tantamount to thermal fatigue, as will be pointed out subsequently.

Strains and Thermal Fatigue

Figure 8(a) indicates the approximate magnitudes of equivalent plastic strain which occurs when the model laminate composite is cooled from 2000° to 80° F (1093.5° to 26.5° C), and figure 8(b) indicates the approximate magnitudes of plastic strain when the model laminate composite is heated from 80° to 2000° F (26.5° to 1093.5° C). Values of plastic strain are plotted as a function of the volume fraction of matrix. When values become small, plastic strain is plotted as dashed lines to indicate that elastic strain values may be significant. Maximum plastic strains as great as about 0.025 have been obtained for either constituent when the composite is cooled or heated from an initial stress-free state. A complete heat-cool cycle can therefore produce a strain range as large as about 0.025 in either constituent. At volume fractions of matrix V_m up to about 0.80, the strain is essentially occurring in the matrix constituent. With higher values of V_m ($\gtrsim$0.85), the relative amount of reinforcement decreases to the point where the unit stress in the reinforcement is sufficiently high to cause essentially all the strain to take place in the reinforcement. Substantial strain will occur in either the matrix or reinforcement; if it does not occur in the one, it can occur in the other.

Data published in references 14 to 16 indicate that steels and alloys can fail in about 1000 cycles when exposed to a thermally induced total strain range of 0.02. Values of strain shown in figure 8 for the model laminate composite produce plastic strain ranges that are of the magnitude just noted; hence material failure may occur in about 1000

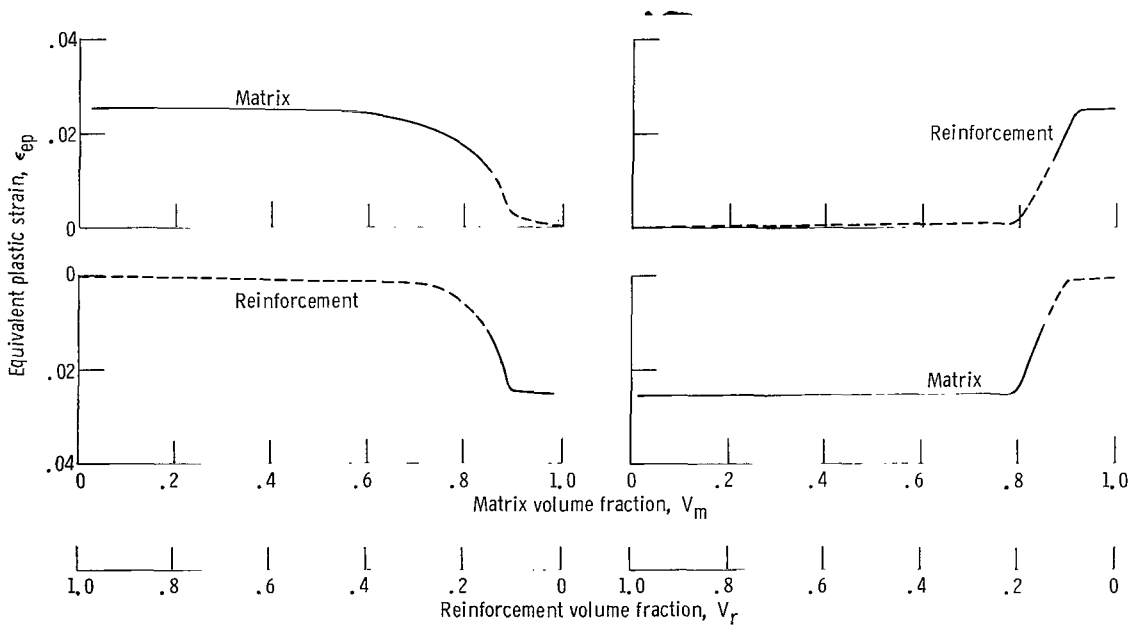

(a) Cooled from 2000° to 80° F (1093.5° to 26.5° C). (b) Heated from 80° to 2000° F (26.5 to 1093.5° C).

Figure 8. - Equivalent plastic strains calculated for model tungsten - 80Ni+20Cr composite.

thermal cycles. The actual number of cycles to failure depends, of course, on test conditions, including material, the relative amounts of elastic and plastic strain, maximum cycle temperature, dwell time at temperature, and, certainly, total strain.

Of cogent interest are the results obtained in an experiment conducted on S-816 alloy gas turbine blades run in a J-47 engine (ref. 17). These blades developed leading-edge cracks after 85 normal start-stop cycles (i.e., heat-cool cycles), involving a thermal gradient of 840° F (450° C) at the leading-edge of the blades. Because of this temperature gradient, the hotter leading edge was constrained from expanding and was compressively strained during heating. The reverse took place upon cooling. The number of cycles to initiate cracking was lessened by introducing periods of normal operation. In a subsequent paper (ref. 18) the elastic strain imposed upon the leading edge of these blades, was calculated to be somewhat less than 0.004. Thus a total strain range of about 0.004 may have been imposed on these blades during a start-stop cycle.

Laboratory test data indicate relatively rapid thermal fatigue damage (i.e., failure in 1000 cycles) for numerous alloys subjected to strain ranges on the order of 0.02. However, in an actual application, a calculated elastic strain range of about 0.004 was associated with thermal fatigue cracking in 85 heat-cool cycles; it may be speculated that creep (i.e., dwell time under stress) may have been a contributing factor in causing the aforementioned cracking. The preceding data and conjecture very strongly suggest that, when the total strain range approaches a magnitude of 0.02 per cycle, thermal fatigue failure may ensue in relatively few cycles (i.e., 1000). The question may also be asked whether or not any losses in mechanical properties may occur prior to any visible material failure; this may be particularly important in regard to the reinforcement material. Thus the use of sheet- or foil-reinforced composites (or fiber-reinforced composites with multidirectional plies) might pose thermal fatigue problems since, in actual usage where thermal cycling might be involved, the strain ranges encountered may be a magnitude sufficiently high to cause material or mechanical property deterioration.

(The thermal expansion of a fiber-reinforced ply or tape can depend on direction, being least in the direction of the fiber if the fibers have the lower coefficient of expansion and being greatest in the direction orthoganal to that of the fibers. Therefore, two fiber-reinforced plies, joined to each other so that the fibers in one ply were at some angle to the fibers in the other ply, would be analogous to alternate sheet or foil of differing thermal expansivities. The type of analysis derived in this study for sheet and foil composites would then be applicable to this particular type of composite insofar as average stresses and strains are concerned.)

Elastic Shear Stress

The calculated peak elastic shear stresses resulting from the cooling or heating of the stress-free model laminate composite are shown in figure 9. These values are shown as a function of the volume fraction of constituent. These stresses occur very near free edges and diminish as one moves away from the edge. The calculated stresses are conservative when $V_r < 0.5$ (see appendix F). On cooling, maximum shear stresses of about 140 ksi (965 MN/m^2) occur at $V_m \approx 0.7$; over the range of $0.2 < V_m < 0.9$, the shear stresses are above 100 ksi (689 MN/m^2). On heating, the maximum peak shear stresses approach 40 ksi (276 MN/m^2) at $V_m \approx 0.8$ and are in excess of 20 ksi (138 MN/m^2) over the range of $0.2 < V_m < 0.9$. Assuming the shear strength to be one-half the tensile strength, the shear strengths may be estimated to be 60 and 2.5 ksi (415 and 17.3 MN/m^2) for the 80Ni+20Cr alloy at 80° and 2000° F (26.5° and 1093.5° C), respec-

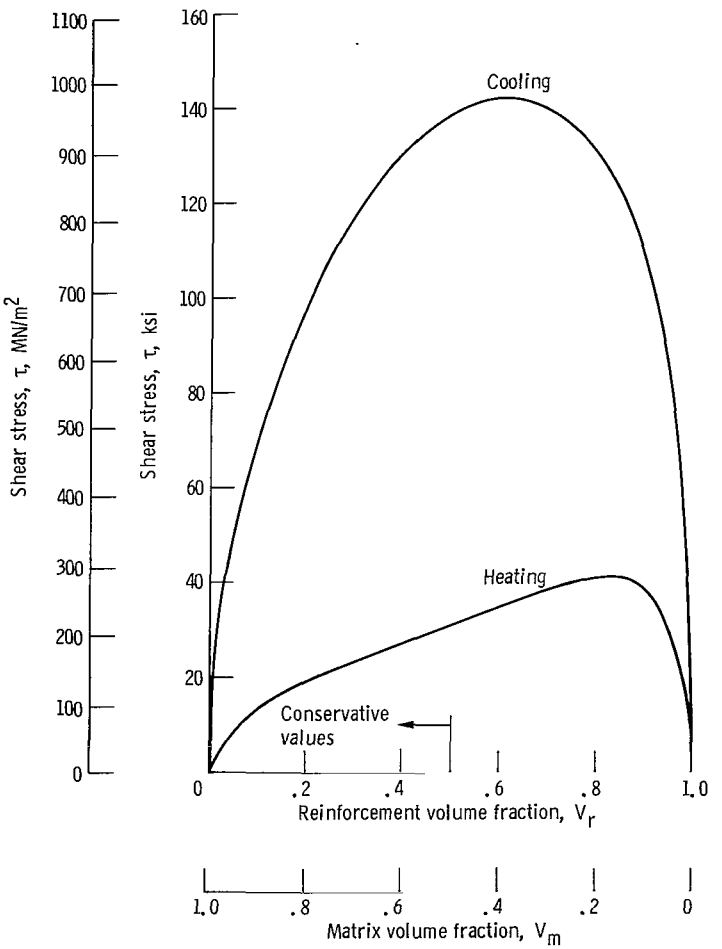

Figure 9. - Peak elastic shear stresses calculated for matrix of tungsten - 80Ni+20Cr laminate composite after heating or cooling between 80° and 2000° F (26.5° and 1093.5° C).

tively. These estimates of shear strength are based on the tensile values shown in figure 7. Thus, it is possible that shear failure could occur in the matrix (or at the interface) particularly over the range of volume fractions of matrix that might be used in practice.

An observation of potential importance may be made. From an inspection of table III, it may be seen that the ultimate tensile strengths of a number of candidate matrix materials is a maximum of about 160 ksi (1104 MN/m^2) at room temperature and about 80 ksi (551 MN/m^2) at 2000° F (1093.5° C). If shear strengths are estimated to be one-half the tensile strengths, shear strengths for matrix materials may approximate 80 ksi (551 MN/m^2) at room temperature and 40 ksi (276 MN/m^2) at 2000° F (1093.5° C). Furthermore, the elastic moduli of many potential matrix materials (see table IV) are similar to or greater than that of 80Ni+20Cr so that the shear moduli would be expected to be similar or greater. Thus, there is a likelihood that the peak shear stresses in many possible matrix materials will exceed their shear strengths.

If plastic deformation occurs rather than fracture, the stresses in the matrix will be less than calculated, but the effect of yielding (particularly cyclic yielding) on bond integrity is not known and repeated yielding of the matrix due to shear stress may cause bond separation or degradation.

A very important point can be made; namely, if discontinuities are introduced into the composite (i.e., if the composite is altered by machining or any other process), free edges may be introduced. Because the highest thermally induced shear stresses occur at or near free edges, these modifications can introduce more potential shear failure sites into the material. Thus, from this particular standpoint, changes in cross section, cutouts, contours, reinforcement or matrix breaks, porosity in the matrix, etc., are all potentially deleterious.

EXPERIMENTAL STUDY OF LAMINATES

A study of limited scope was conducted to obtain indications of whether readily apparent damage could be induced in reinforced sheet or foil laminate composites. The calculated stresses in the tungsten - 80Ni+20Cr composite model were determined to be sufficiently high to result in tensile, compressive, or shear failure during the first cooling or heating cycle if plastic stress relief did not occur. And should stress relief occur, thermal fatigue might later ensue after a number of heat-cool cycles. Simple heat-cool tests were used to determine whether a relatively few heat-cool cycles could produce readily apparent laminate composite deterioration. There was no intent to necessarily induce thermal fatigue in the event this type of damage should require large numbers of cycles. Heat-cool cycles with very slow heating and cooling rates were used, as well as heat-cool cycles with fairly rapid heating and cooling rates. Thermal gradients would be

minimal for slow heating and cooling rates, if they occurred at all. But in actual use conditions, such as might be encountered in a turbine blade application, rapid heating and cooling could produce temperature gradients and, therefore, produce stresses which are additive to those due to the differences in the thermal expansions of the constituents.

Materials

Commercial tungsten and 80Ni+20Cr sheets and foils were used as the laminae. Table VI shows the thicknesses of the laminae used. The specimens were formed by alternating layers (lamina) of tungsten and 80Ni+20Cr. Six specimens approximately 1- by 3-inch (2.54- by 7.12-cm) thick were tested. Three were as-fabricated (rectangular specimens, fig. 10(a)), and three had the configuration shown in figure 10(b) (contoured specimens). The rectangular specimens were used in the slow heat-cool tests; the contoured specimens in the more rapid heat-cool tests. Both types of specimen had 0.001-, 0.005-, and 0.020-inch (0.0025-, 0.0125-, and 0.050-cm) thick tungsten laminae with corresponding 80Ni+20Cr laminae thicknesses (see table VI). The tungsten laminae were used in the as-received thickness; the 80Ni+20Cr were obtained in 0.001- and 0.005-inch (0.0025- and 0.0125-cm) thicknesses, and laminae over 0.005 inch (0.0125 cm) thick were made by using multiple layers of 0.005-inch (0.0125-cm) thick foils.

The volume fraction of tungsten was about 0.50 in all instances. The different foil thicknesses were used because they were conveniently available and because any possible

TABLE VI. - SPECIMEN DETAILS

[All thickness values are approximate.]

Specimen shape	Tungsten laminae			80Ni+20Cr laminae			Total number of laminae	Specimen thickness	
	Thickness		Number	Thickness		Number		in.	cm
	in.	cm		in.	cm				
Rectangular[a]	0.001	0.0025	20	0.001	0.0025	21	41	0.041	0.1
	.005	.0125	10	.005	.0125	11	21	.105	.263
	.020	.050	4	[b].020	[b].050	5	9	.180	.457
Contour[c]	0.001	0.0025	20	0.001	0.0025	21	41	0.041	0.1
	.005	.0125	10	.005	.0125	11	21	.105	.263
	.020	.050	2	(d)	(d)	3	5	.080	.200

[a]Used for slow heat-cool cycles. See fig. 13(a).

[b]Four 0.005-in. (0.0125-cm) thick 80Ni+20Cr foils were used to form the 0.020-in. (0.0125-cm) thick lamina.

[c]Used for rapid heat-cool cycles. See fig. 13(b).

[d]The outer 80Ni+20Cr laminae were 0.010 in. (0.025 cm) thick (two 0.005-in. (0.0125 cm) foils); the inner lamina was 0.020 in. (0.050 cm) thick (four 0.005-in. (0.0125-cm) foils).

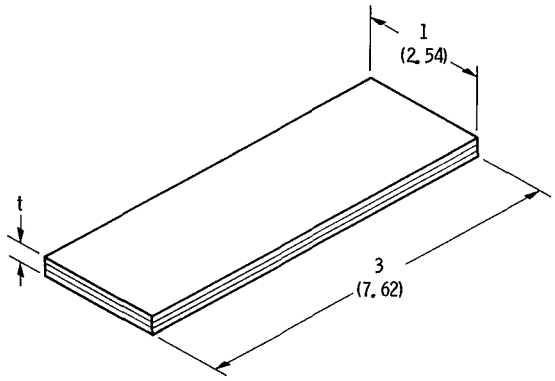

(a) Rectangular specimen used for slow heat-cool tests.

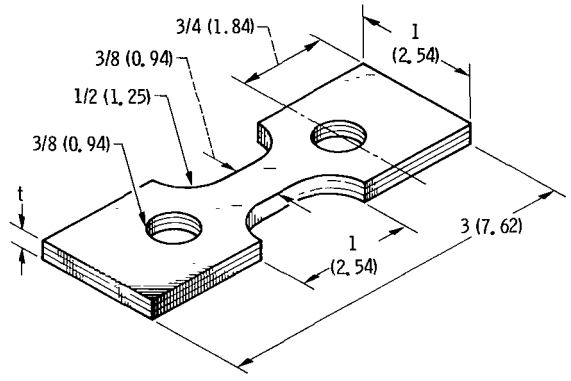

(b) Contour specimen used for rapid heat-cool tests.

Figure 10. - Configurations of heat-cool test specimens. (Dimensions are in inches (cm).)

effect of lamina thickness on composite susceptibility to damage was of interest. All specimens were consolidated (bonded) by vacuum hot pressing for 4 hours at 1800° F (980° C) and 4 ksi (28 MN/m^2) or better. Specific details of the specimens are given in table VI.

Procedure

The specimens having the rectangular profile were exposed simultaneously (i.e., three at a time); they were slowly heated in a vacuum furnace for 2 hours to 2000° F (1093.5° C) and allowed to remain at this temperature for 2 hours. The specimens were then slowly cooled to room temperature for 2 hours. The vacuum was 10^{-5} torr (13 MN/m^2) or better. They were inspected after each heat-cool cycle, using magnifications up to ×150.

The contoured specimens (fig. 10(b)) were each placed into a separate heat treating envelope. Each specimen was placed in a furnace which had been preheated to 1600° F

(877° C) and allowed to remain in the furnace for 15 minutes. Each specimen was given its first cooling cycle by being immersed in a container of water. But the envelopes became filled with water, and subsequent cooling was accomplished by placing the specimen on a metal plate which was at ambient temperature. The specimen having the 0.020-inch tungsten laminae failed after the first cooling cycle and was not tested further. The 1600° F (877° C) furnace temperature was used because of the furnace temperature limitations and because it was desired to minimize specimen oxidation which might occur.

Varying numbers of cycles were used in both the slow and fast cycle tests in order to obtain a balance between observable effects and ready availability of evaluation apparatus.

Results and Discussion

Slow heat-cool cycles. - The results of the slow heat-cool cycles are summarized in table VII(a). The composite with the 0.020- (0.050-cm) thick laminae, exhibited delamination after the first cycle and progressive delamination up to the third cycle. The damage appeared to be essentially stabilized at this time. The specimen with the 0.005-inch (0.0125-cm) laminae exhibited microdamage after 11 heat-cool cycles. The specimen with the 0.001-inch (0.0025-cm) laminae did not exhibit any observable damage through the 11th heat-cool cycle. The appearance of the specimens after 11 cycles is shown in figure 11.

Even with very slow heating and cooling, visible damage did occur. The calculated elastic-plastic stresses for the matrix were 7 and 76 ksi (48.2 and 523 MN/m^2) on heating and cooling, respectively, assuming that relaxation did not occur. The calculated stresses in the reinforcement were also 7 and 76 ksi (48.2 and 523 MN/m^2) on heating and cooling, respectively. The calculated plastic strain range in the matrix was about 0.025 per heat-cool cycle. The calculated elastic shear stress in the matrix was 30 and 140 ksi (208 and 965 MN/m^2) during heating and cooling, respectively. With a strain range of about 0.025, thermal fatigue damage might be expected in less than 1000 cycles, and, possibly, thermal fatigue damage actually occurred in the specimen with the 0.005-inch (0.0125-cm) laminae.

Rapid heat-cool cycles. - The results of this experimentation are summarized in table VII (b). The specimen containing the 0.020-inch (0.050-cm) tungsten laminae was completely unbonded after the first cycle. The specimen containing the 0.005-inch (0.0125-cm) tungsten laminae, which showed no damage after the first heat-cool cycle, was very badly damaged after two more cycles. The laminate specimen containing the 0.001-inch (0.0025-cm) tungsten laminae exhibited incipient laminae separation after six heat-cool cycles. The appearance of each of these specimens at the end of its respective final test cycle is shown in figure 12. The calculated laminae stresses and strains correspond to those previously indicated for the slow-cool specimens. Because

TABLE VII. - RESULTS OF FURNACE THERMAL CYCLING

(a) Slow cool

Laminae thickness				Number of cycles	Results
Tungsten		80Ni+20Cr			
in.	cm	in.	cm		(a)
0.001	0.0025	0.001	0.0025	11	No macroscopically visible damage
0.005	0.012	0.005	0.012	11	Cracking of lamallae - possible delamination
0.020	0.050	0.020	0.050	1	Delamination
				2	Further delamination
				3	Further delamination
				11	Slightly further delamination

(b) Rapid cool[b]

Laminae thickness				Number of cycles	Results
Tungsten		80Ni+20Cr			
in.	cm	in.	cm		(c)
0.001	0.0025	0.001	0.0025	6	Incipient foil separation
0.005	0.0125	0.005	0.0125	3	Foil separation, shear buckling
0.020	0.050	(d)	(d)	1	Sheets unbonded

[a]See fig. 11.

[b]First quench was into water container. Subsequent quenches by air cool on metallic plate at ambient temperature. Specimens were in a 1600° F (877° C) furnace for 15 min and then removed for cooling.

[c]See fig. 12.

[d]See footnote (d), table VI.

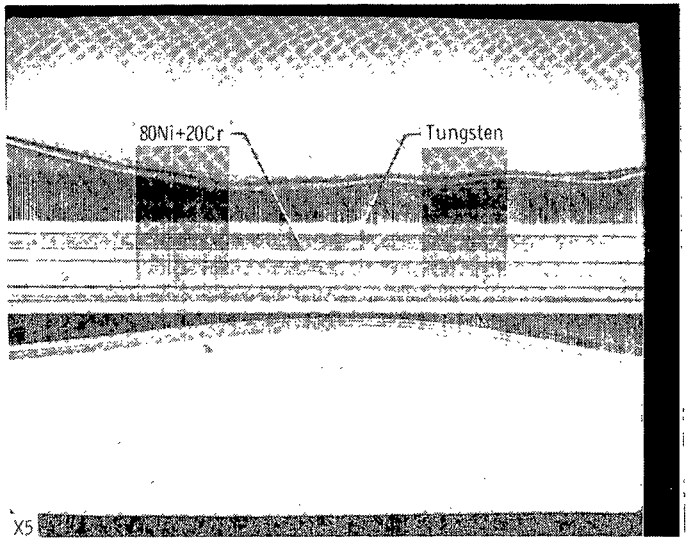

(a) Tungsten lamina thickness, 0.020 inch (0.050 cm). Appearance essentially unchanged from that observed after three cycles. Note gross delamination of outer elements and separation of inner elements.

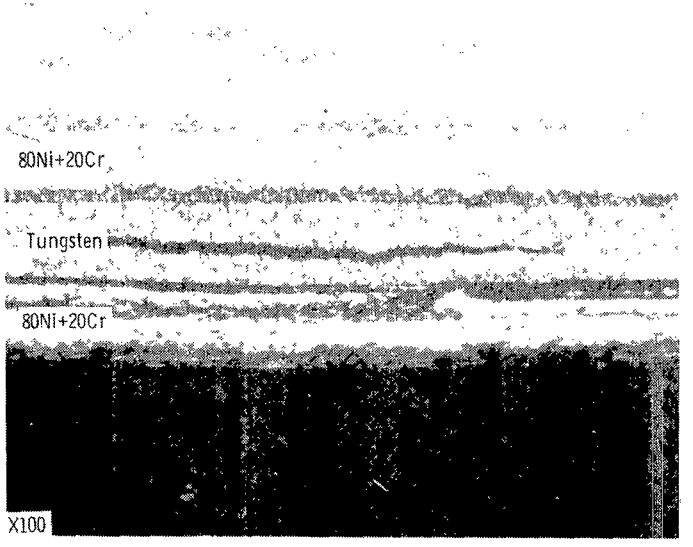

(b) Tungsten lamina thickness, 0.005 inch (0.0125 cm). Note cracking of both tungsten and 80Ni+20Cr laminae. There is indication of bond separation.

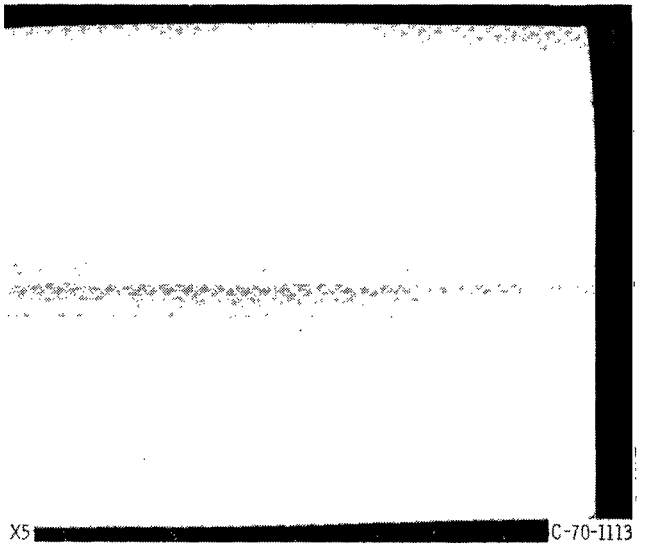

(c) Tungsten lamina thickness, 0.001 inch (0.0025 cm). No discernable damage.

Figure 11. - Tungsten - 80Ni+20Cr composite after 11 slow heat-cool cycles to and from 80° and 2000° F (26.5° and 1093.5° C). Tested in as-hot-pressed condition. Photographs reduced by 20% in reproduction.

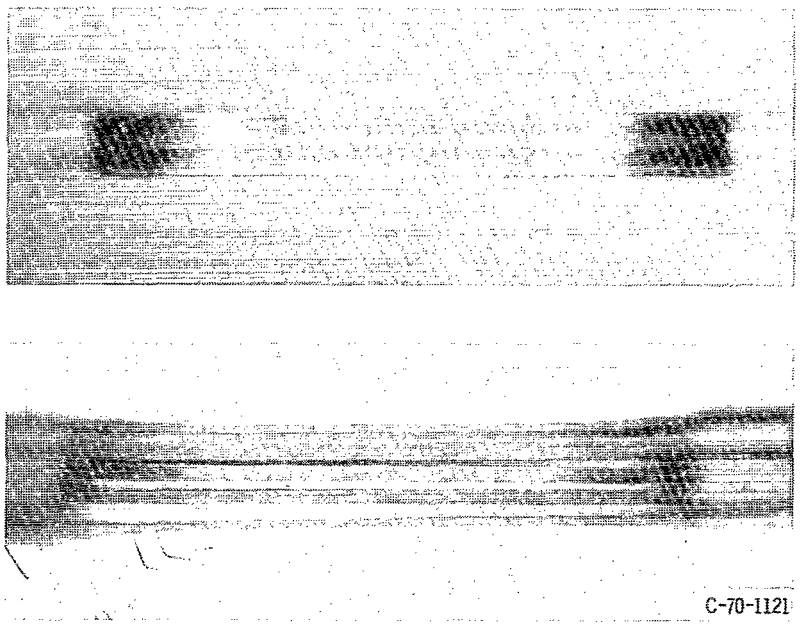

(a) Tungsten lamina thickness, 0.020 inch (0.050 cm); after one cycle.

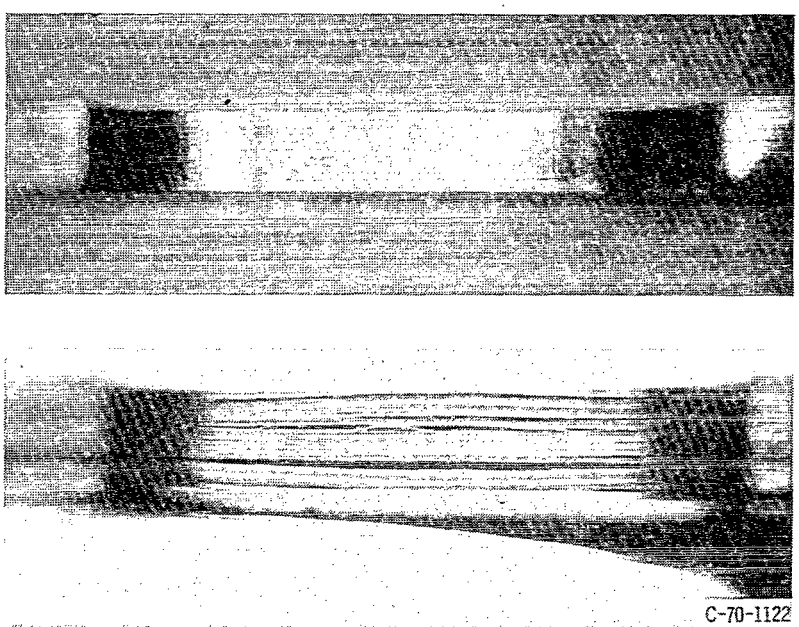

(b) Tungsten lamina thickness, 0.005 inch (0.0125 cm); after three cycles. Note shear failure at interface, breaking, and damage to tungsten lamina.

Figure 12. - Tungsten - 80Ni+20Cr composite before (top)and after (bottom) rapid heat-cool cycles to and from room temperature and 1600° F (877° C). Specimen tested in as-hot-pressed condition. X2.

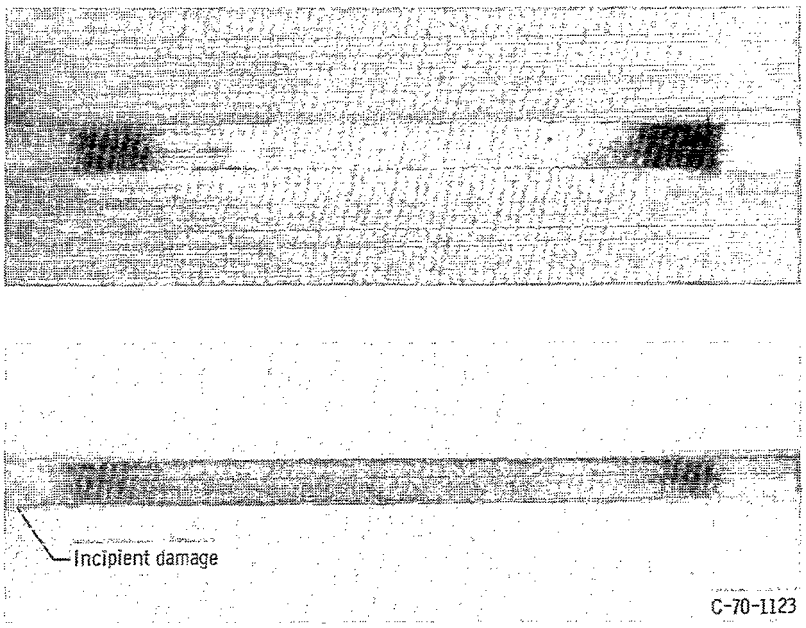

(c) Tungsten lamina thickness, 0.001 inch (0.0025 cm); after six cycles.

Figure 12. - Concluded.

of the relative rapidity of temperature change, there is a possibility of introducing thermal gradients and concommitant additive stresses, so that the end result in these particular tests are not necessarily attributable to thermal expansion differences alone. Actually, however, rapid temperature changes could well be encountered in practical applications, so that these particular results obtained in the relatively rapid heat-cool study could indicate what might actually be encountered.

Regardless of whether the heating and cooling was slow or rapid, the greatest observed structural damage occurred to the specimens with the thickest laminae, and the least to the specimens with the thinnest laminae. In both instances the 0.020-inch (0.050-cm) laminae specimen sustained delamination, which indicates a predominance of shear effects. Inspection of the equation for shear stress (eq. (3) or (B21)) indicates that the shear stress decreases more rapidly away from the tip, as the matrix laminae thickness decreases. Thus, the region of high shear stress would be greatest for the 0.020-inch (0.050-cm) thick laminae composites and least for the 0.001-inch (0.0025-cm) thick laminae composites; and it might explain the apparent decreased effect of shear with decreased laminae thickness. Another possible reason for lesser damage in the thinner laminae composites is that a given amount of interdiffusion would involve a relatively larger amount of each lamina. This could tend to lessen the differences between the coefficients of thermal expansion of adjacent lamina and thereby lessen the stresses actually developed. This effect would be greatest for the 0.001-inch (0.0025-cm) laminae composites. Obviously, the more rapid temperature change accelerated the structural damages.

SIGNIFICANCE OF MATHEMATICAL ANALYSIS AND EXPERIMENTAL RESULTS

The mathematical stress analysis and the resulting calculated stresses for the tungsten - 80Ni+20Cr laminate composite indicated that very high tensile, compressive, or shear stresses (in excess of the ultimate tensile and the estimated shear strengths of the materials) could be generated because of the difference in the coefficients of thermal expansion of the constituents and because of a temperature transition between 2000^{o} and 80^{o} F (1093.5^{o} and 26.5^{o} C). The materials combination and the temperature ranges were representative of a genre of composite materials and use-conditions that are being considered for practical application. The high calculated elastic stresses could be meliorated by plastic deformation but the concurrent strains might cause thermal fatigue damage if cyclic heating and cooling were encountered. From an analytical viewpoint, the model system studied seemed prone either to immediate structural damage due to high stresses or to limitations on its endurance due to strain associated with cyclic thermal stresses.

An experiment involving relatively few heat-cool cycles applied to tungsten - 80 Ni+20Cr laminate composites resulted in damage (whether the heating and cooling rates be slow or rapid) for laminae thicknesses that might be of practical interest. The extent of this damage was greater with increased laminae thicknesses and with more rapid heating and cooling rates.

Thus, sheet or foil laminate composites may be prone to damage as the result of high thermally induced stresses arising from differences in coefficients of thermal expansion of the constituents and exposure to one or more temperature transitions.

FIBER COMPOSITES

STRESSES IN FULL-LENGTH FIBER-REINFORCED COMPOSITES

Fiber-reinforced composites have been arbitrarily catagorized as being high volume fraction if they have between 65 and 90 percent fiber and low volume fraction if they have less than 65 percent fiber content. The 90 percent figure corresponds to the theoretical packing limit of circular fibers. The 65-percent figure is about the minimum amount of reinforcement assumed to be usually associated with high volume-fraction composites.

The low volume-fraction fiber composites were assumed to be amenable to analysis using thick shell theory, and the high volume-fraction fiber composites were assumed to be in a state of hydrostatic stress. A rigorous mathematical analysis incorporating the effect of volume fraction of fiber and related constraints was beyond the scope of this study.

High Volume-Fraction Composites ($0.65 < V_r < 0.90$)

Assumptions. -

(1) The fibers are well bonded to the matrix.

(2) Each constituent is homogeneous and isotropic, and has the same Poisson's ratio.

(3) A hydrostatic stress state exists within each constituent of the composite; that is, $\sigma_\theta = \sigma_R = \sigma_x$. The hydrostatic stress state is the result of a sufficiently high volume fraction of fiber so that there is stress interaction between matrix and fibers.

(4) Tensile and compressive stresses are uniform within the breadth of the respective constituents.

(5) The fibers are in a hexagonal array.

(6) There is no interphase region.

(7) End effects are neglected.

Mechanism of stress generation. - A model is shown in figure 13. Figure 13(a) illustrates a complete composite containing many full-length fibers. Figure 13(b) represents an element of this composite comprising a fiber and an "associated" shell of matrix. The polar coordinate system used is shown in figure 14. The fiber and matrix have different coefficients of thermal expansion, and the composite is assumed to have been consolidated at elevated temperature and cooled to room temperature. Because of

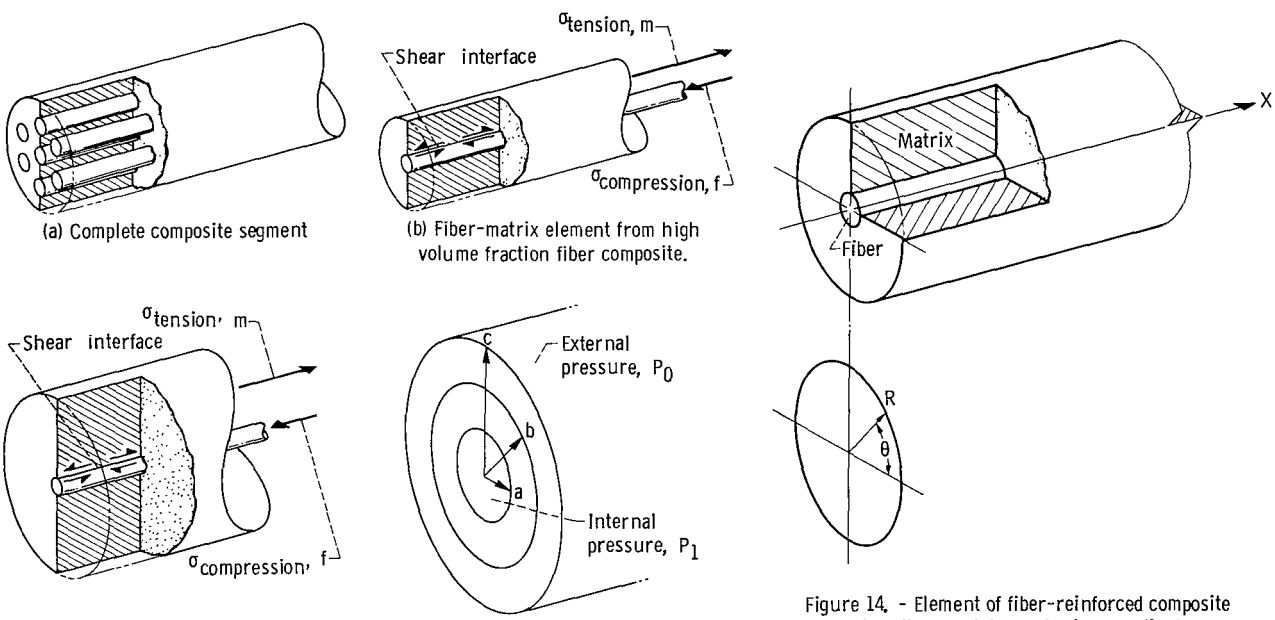

Figure 13. - Fiber-reinforced composites.

Figure 14. - Element of fiber-reinforced composite showing fiber, matrix, and polar coordinate system.

the greater thermal contraction of the matrix, it will contract about the fiber. Stresses will be introduced into the fiber and the matrix. These stresses will be in the longitudinal (as shown), radial, and tangential directions. If a consolidated composite is heated, stresses of an opposite sign to those produced on cooling will result. Stresses and strains will be produced on each subsequent heating or cooling. The derivation of equations for longitudinal, radial, and tangential stress is given in appendix C. The resultant equations are as follows:

$$\sigma_{xm} = \sigma_{Rm} = \sigma_{\theta m} = \frac{V_r E_r E_m (\alpha_r - \alpha_m)\Delta T}{(V_r E_r + V_m E_m)(1 - 2\nu)} \tag{5}$$

$$\sigma_{xr} = \sigma_{Rr} = \sigma_{\theta r} = \frac{V_m E_m E_r (\alpha_m - \alpha_r)\Delta T}{(V_r E_r + V_m E_m)(1 - 2\nu)} \tag{6}$$

There will be no plastic deformation since it has been assumed that a hydrostatic stress state exists.

Low Volume-Fraction Composites

Assumptions. -

(1) Matrix reinforcement are perfectly bonded.

(2) Matrix and reinforcement are, respectively, homogeneous and isotropic and have the same Poisson's ratio.

(3) There is no stress interaction between matrix and neighboring fibers; thus, the thick-wall cylinder theory applies.

(4) The fibers are in a hexagonal array.

(5) There is no interphase region.

(6) End effects are neglected.

Mechanism of stress generation. - The model is represented in figure 13, an element of which is illustrated in figure 13(c). The coordinate system is shown in figure 14. The composite, consisting of matrix and fibers with different coefficients of thermal expansion is assumed to have been consolidated at elevated temperature and cooled to room temperature. Both constituents are initially the same length and after cooling are again of equal lengths. This will generate longitudinal (as shown), radial, and tangential stresses in fiber and matrix as before, but, because of assumption (3), plastic flow can take place. If the composite were stress free at room temperature and heated, stresses

would again be generated, but of opposite signs. The derivations are presented in appendix D and the resulting equations are

$$\sigma_{mR} = -p_i \tag{7}$$

$$\sigma_{m\theta} = \frac{\beta^2 + 1}{1 - \beta^2} p_i \tag{8}$$

$$\sigma_{rR} = -p_o \tag{9}$$

$$\sigma_{r\theta} = -p_o \tag{10}$$

$$\sigma_{mx} = \frac{V_r E_r E_m(\alpha_r - \alpha_m)\Delta T + V_r \nu p\left(\frac{2\beta^2}{1 - \beta^2} E_r + 2E_m\right)}{V_r E_r + V_m E_m} \tag{11}$$

$$\sigma_{rx} = \frac{V_m E_r E_m(\alpha_m - \alpha_r)\Delta T - V_m \nu p\left(\frac{2\beta^2}{1 - \beta^2} E_r + 2E_m\right)}{V_r E_r + V_m E_m} \tag{12}$$

where

$$p = p_i = p_o = \frac{(\alpha_m - \alpha_r)\Delta T\, E_m E_r(1 - \beta^2)}{E_r\left[\beta^2(1 - \nu) + (1 + \nu)\right] + E_m(1 - \beta^2)(1 - \nu)} \tag{13}$$

$$\beta^2 = \left(\frac{b}{c}\right) \tag{14}$$

and b and c are fiber and associated matrix radii, respectively, as shown in figure 13(d). Equations (7) and (8) give stresses at the fiber-matrix interface; the matrix stress are theoretically the largest at this point.

Equations (7) to (12) yield elastic stress values but may be used to obtain estimates of elastic-plastic stresses and strains as discussed in appendix C.

ELASTIC SHEAR STRESSES IN FULL-LENGTH FIBER-REINFORCED COMPOSITES

Assumptions

An equation for shear stress may be derived in a manner analogous to that used for the laminate composite. All previous assumptions made for the laminate composite still apply with the exceptions or additions that

(1) A triaxial rather than a biaxial stress-state exists.

(2) The fibers are in a hexagonal array.

(3) The interfiber distance is equal to or less than the fiber diameter; this corresponds to $V_r > 0.23$.

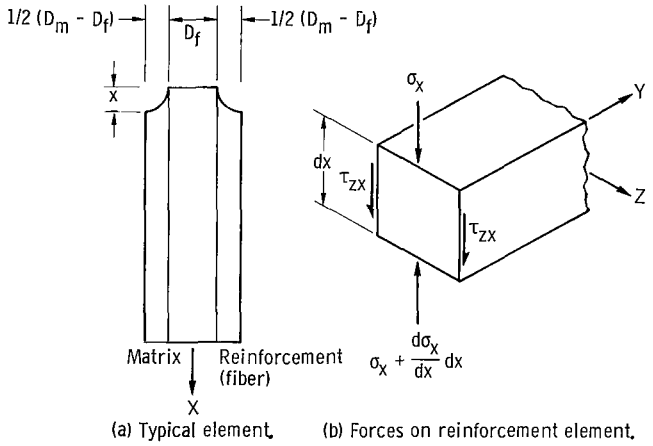

Figure 15. - Element of fiber reinforced composite and forces acting on reinforcement (i.e., fiber).

Mechanism of Stress Generation

A plane section through the fiber and its associated cylinder of matrix may be represented by figure 15. The comments made regarding stress generation (p. 7) apply, and the actual derivation is given in appendix E. The resulting equation for elastic stress is

$$\tau_{mx} = \frac{(\alpha_m - \alpha_r)\Delta T\, 2G_m e^{-\lambda x/(D_m - D_r)}}{\left[1 + \frac{(1 - \nu K)_m}{(1 - \nu K)_r}\left(\frac{E_r}{E_m}\right)\frac{D_r^2}{\left(D_m^2 - D_r^2\right)}\right]\lambda} \tag{15}$$

where

$$\lambda_2^2 = \frac{8G_m(1 - \nu K)_m(D_m - D_r)}{D_r} \tag{16}$$

CALCULATION OF RESIDUAL THERMAL STRESSES AND STRAINS IN MODEL FIBER-REINFORCED COMPOSITE

Residual stresses have been calculated for a model fiber-reinforced composite containing tungsten fibers in a 80Ni-20Cr matrix, as was the case for the laminate composites. Conditions A and B (p. 9) will be used again as will the respective material properties as shown in table I. The purpose of these calculations is to obtain representative stress and strain magnitudes for the model composite, and these values will be applicable to other materials combinations having similar coefficients of thermal expansion, Poisson's ratios, yield strengths, and elastic moduli. The results of the calculations are shown in figures 16 to 21.

Tensile and Compressive Stresses in High-Volume-Fraction Fiber-Reinforced Composites

Cooling. - Fiber contents ranging from an arbitrary 0.65 to 0.90 volume fraction (the maximum theoretical fiber content for circular fibers is 90.3 percent) have been assumed to comprise high volume-fraction fiber-reinforced composites. Stresses for composites with $V_r > 0.90$ have been indicated by dashed lines since V_r cannot exceed about 0.90 for circular fibers. Figure 16(a) indicates that on cooling, the tensile stress (i.e., σ_θ, σ_R, or σ_z) in the matrix can range from about 750 to about 600 ksi (5170 to 4150 MN/m^2). Tensile stresses of this magnitude should cause fracture of the matrix (unless yielding occurs). The calculated compressive stress in the fibers may be as high as 350 ksi (2430 MN/m^2) (for the 0.65 volume fraction fiber composites), and compressive stresses of this magnitude should not cause any immediate harm to the tungsten reinforcement.

Heating. - Figure 16(b) indicates that matrix compressive stresses (i.e., σ_θ, σ_R, and σ_x) as high as 200 ksi (1378 MN/m^2) may be generated on heating. These may fracture the matrix (unless relieved by plastic yielding). Tensile stresses as great as 100 ksi (689 MN/m^2) may be generated in the reinforcement. Stresses of this magnitude would probably fracture the tungsten fibers (unless plastic deformation occurred).

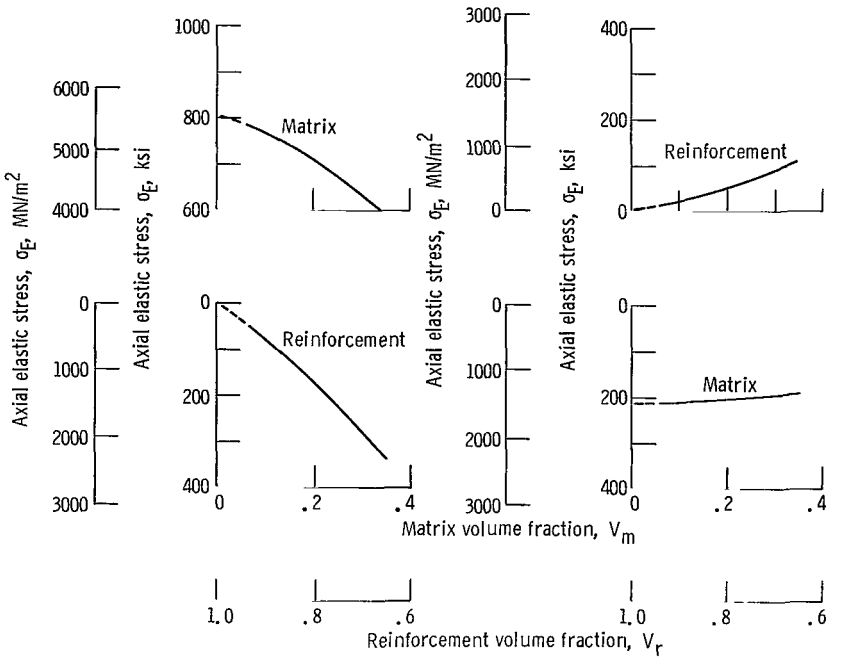

Figure 16. - Axial elastic stresses ($\sigma_X = \sigma_\theta = \sigma_R$) calculated for model high-volume-fraction ($0.65 < V_r < 0.90$) tungsten - 80Ni+20Cr-matrix fiber composites.

Tensile and Compressive Stresses in Low-Volume-Fraction Fiber-Reinforced Composites

Cooling. - Figure 17(a) indicates that longitudinal compressive stresses as great as about 700 ksi (4716 MN/m^2) can be generated in the fibers and tensile stresses as great as about 250 ksi (1722 MN/m^2) could be generated in the matrix. Transverse tensile stresses (fig. 17(b)) ranging from about 250 to about 380 ksi (1722 to 2600 MN/m^2) could be developed in the matrix. Transverse compressive stresses as high as about 250 ksi (1722 MN/m^2) could be developed in the matrix and reinforcement with low matrix volume fractions; these stresses decrease to about 75 ksi (516 MN/m^2) with a reinforcement volume fraction of about 0.65. The reinforcement stresses might not be damaging, but the matrix stresses could cause fracture on first cooldown if not relieved by plastic flow.

Heating. - Figure 18(a) indicates longitudinal fiber tensile stresses as high as about 450 ksi (3100 MN/m^2) at small reinforcement volume fractions; these stress values decrease to about 40 ksi (276 MN/m^2) with an increase in the reinforcement volume fraction to about 0.65. The compressive stress in the matrix increases to about 80 ksi (55 MN/m^2) as the reinforcement volume fraction increases to about 0.65. The trans-

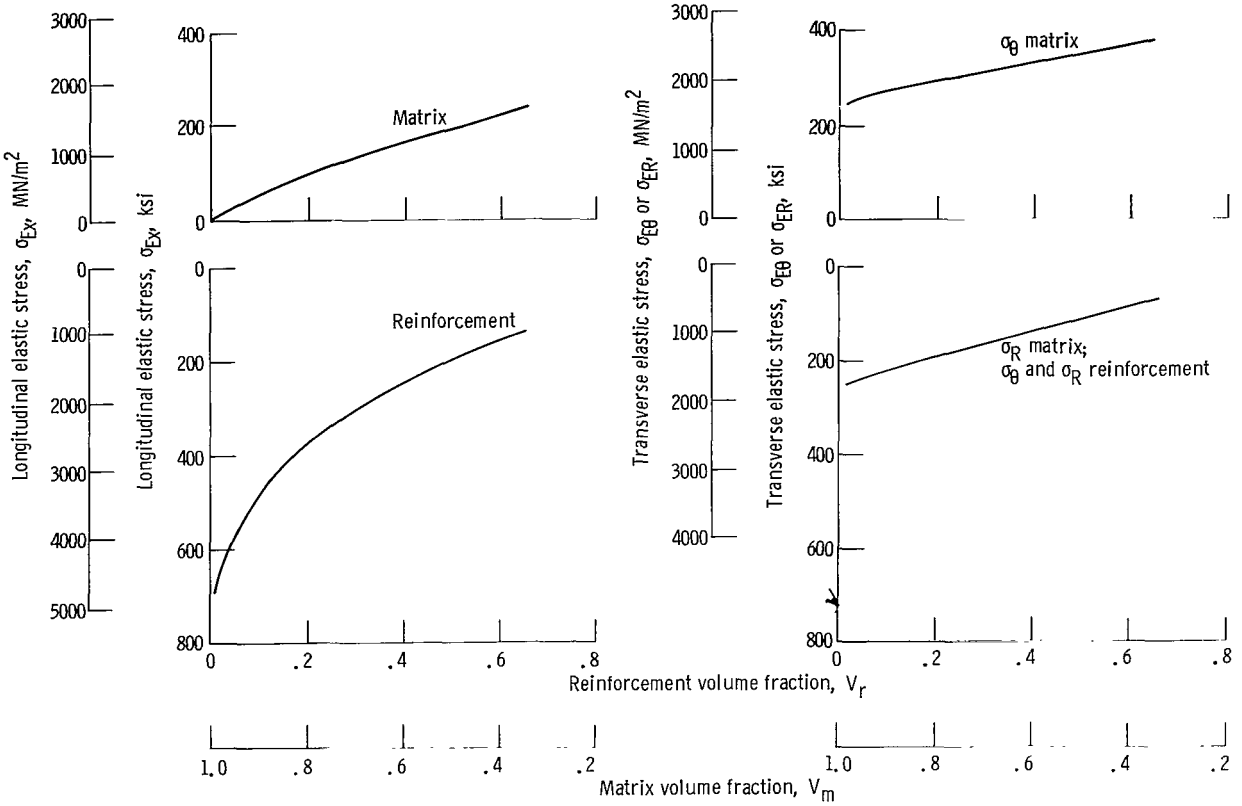

Figure 17. - Elastic stresses calculated for model low volume fraction ($V_r < 0.65$) tungsten-fiber-reinforced - 80Ni+20Cr-matrix composites. After cooling from 2000° to 80° F (1093.5° to 26.5° C).

verse compressive stresses (fig. 18(b)) in the matrix increase from about 75 ksi (503 MN/m^2) at low reinforcement volume fractions to about 100 ksi (689 MN/m^2) at matrix volume fractions of about 0.65. The reinforcement and matrix tensile stresses decrease from about 80 to about 20 ksi (551 to 138 MN/m^2) over this same reinforcement volume-fraction interval. Microfracture of either constituent could occur upon first heating at some of these stress levels unless relieved by plastic deformation.

Tensile and Compressive Stresses in Low-Volume-Fraction Fiber-Reinforced Composites on Assumption of Elastic-Plastic Deformation

These stresses and strains were calculated using the method and assumptions described in appendix D.

Cooling. - Equivalent stresses were calculated and are shown in figure 19. A maximum compressive stress in the fiber of about 300 ksi (2070 MN/m^2) may be obtained at

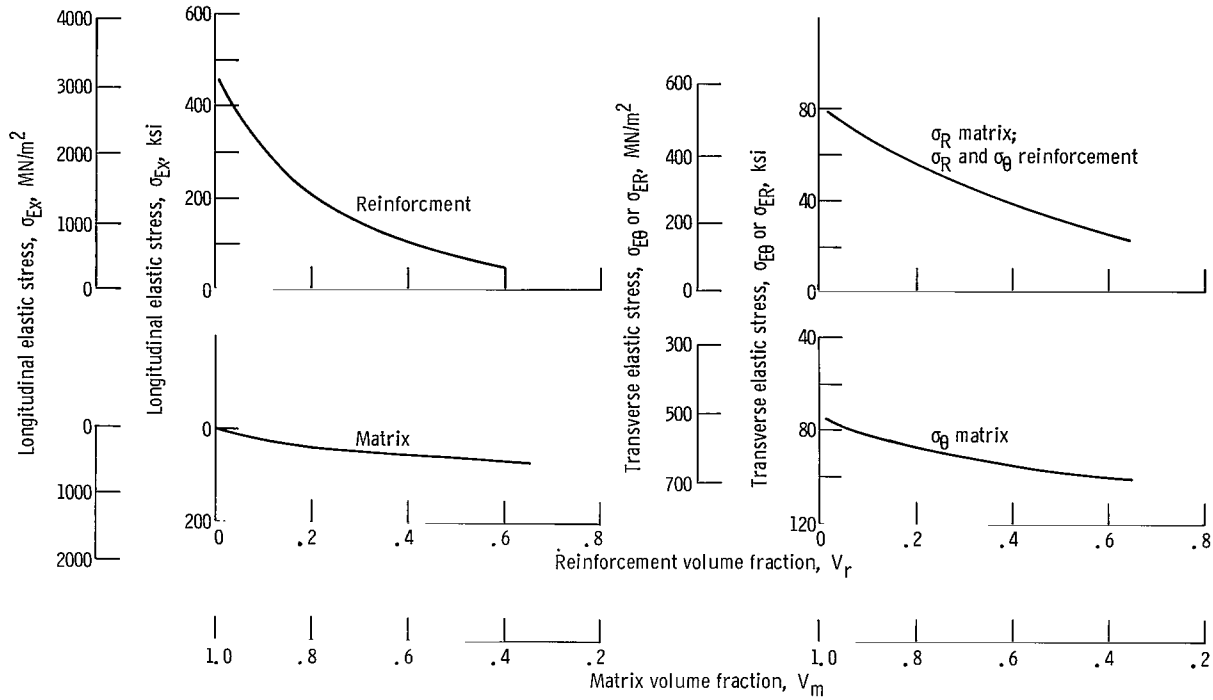

(a) Longitudinal stress. (b) Transverse stress calculation for interface.

Figure 18. - Elastic stresses calculated for model low volume fraction ($V_r < 0.65$) tungsten-fiber-reinforced - 80Ni+20Cr-matrix composites. After heating from 80° to 2000° F (26.5° to 1093.5° C).

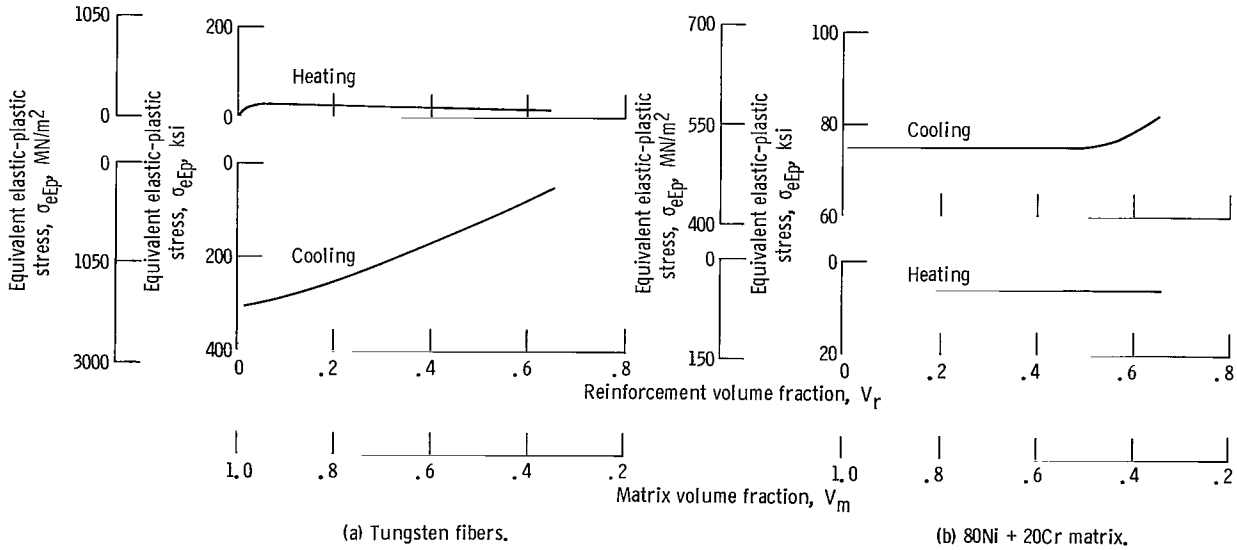

(a) Tungsten fibers. (b) 80Ni + 20Cr matrix.

Figure 19. - Equivalent elastic-plastic stresses calculated for model low volume fraction ($V_r < 0.65$) tungsten-fiber-reinforced - 80Ni + 20Cr-matrix composite. After heating or cooling between 80° and 2000° F (26.5° and 1093.5° C).

low reinforcement volume fractions. With reinforcement volume fractions of about 0.65, the stress decreases to about 50 ksi (345 MN/m^2). The matrix tensile stress is about 75 ksi (518 MN/m^2) for the low reinforcement volume-fraction composites. This stress increases to about 80 ksi (551 MN/m^2) for reinforcement volume fractions approaching 0.65.

Heating. - Inspection of figure 19 indicates that the maximum tensile fiber stress will be about 35 ksi (220 MN/m^2) for low volume-fraction composites decreasing to about 20 ksi (138 MN/m^2) for a fiber fraction of about 0.65. The matrix compressive stress will be about 6 ksi (42 MN/m^2) for composites with fiber volume fractions up to 0.65.

Strains and Thermal Fatigue in Low-Volume-Fraction Fiber-Reinforced Composites

Elastic-plastic equivalent strains are presented in figure 20. The maximum total and plastic strains occurring in the fiber on cooling are about 0.010 and 0.005, respectively, and these values decrease rapidly as the reinforcement volume fraction is increased. The maximum total and plastic strains occurring in the fiber on heating are 0.01 and 0.008, respectively, and also decrease rapidly with increasing reinforcement volume fraction. The total and plastic strains in the matrix are quite similar to each other. On cooling, the matrix plastic strain is about 0.011 up to a reinforcement volume fraction of about 0.50. Above this value of reinforcement, the matrix strain increases rapidly to about 0.033 at a reinforcement volume fraction of 0.65. On heating, the plastic strain in the matrix is about 0.014 and remains at this level, even up to reinforcement volume fractions of 0.65. The strains in the reinforcement may be damaging when the amount of the reinforcement is relatively small (i.e., $V_r < 0.25$). Cyclic strain, as small as 0.004, which may occur when $V_r < 0.25$, was associated with gas turbine blade cracking (refs. 17 and 18) in only 85 thermal cycles. The strains calculated for the matrix are of even greater concern because of their greater magnitude and because they occur for virtually all amounts of fiber content up to $V_r = 0.65$. Further, an appreciable amount of data (refs. 14 to 16), indicates that a cyclic strain range of 0.02 can cause thermal fatigue in 1000 cycles. Since the matrix strain can be on the order of 0.01, matrix endurance could be cycle limited, even if it exceeds 1000 cycles. In actuality, the calculated strains would probably be approached with lower volume fractions of reinforcement, but, as the amount of reinforcement is increased, the amount of strain would become progressively lower, until, at high values of reinforcement volume fraction, there would be essentially complete restraint and structural damage would occur rather than plastic flow.

Obviously, a refractory-metal-fiber-reinforced alloy matrix composite can be

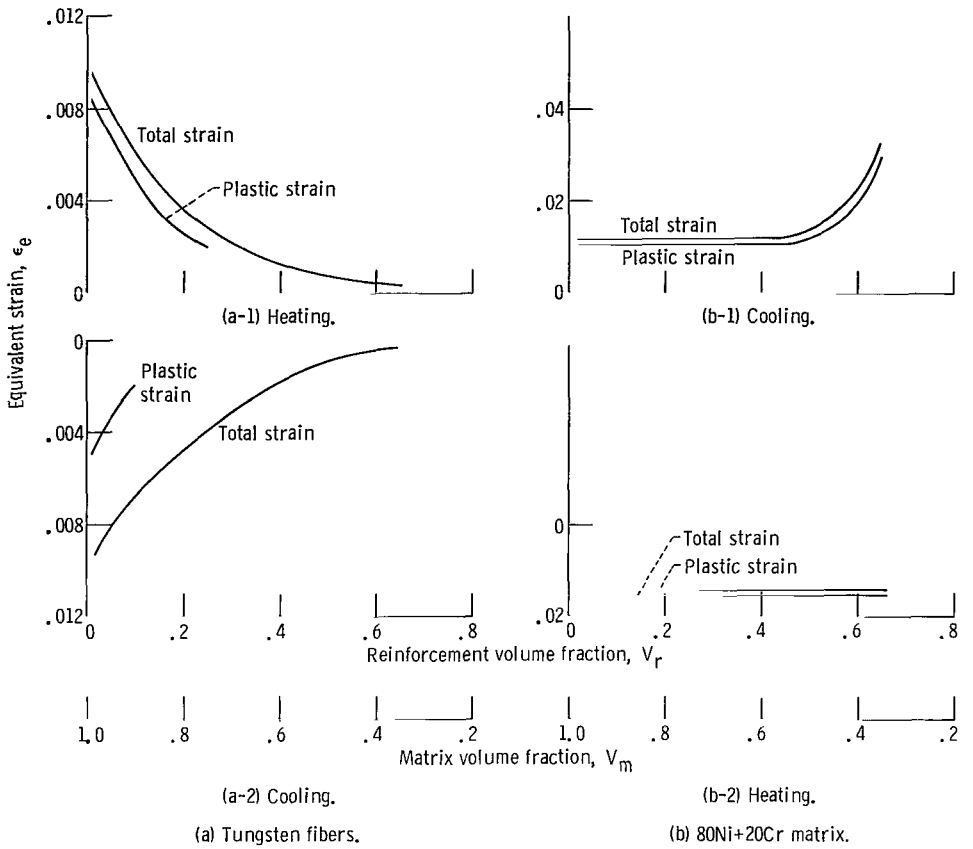

Figure 20. - Equivalent total and plastic strains estimated for model low volume fraction ($V_r < 0.65$) tungsten-fiber-reinforced - 80Ni+20Cr-matrix composite. After cooling between 80° and 2000° F (26.5° and 1093.5° C).

harmed by cyclic thermal stressing. Possible loss of fiber strength or even fracture could occur after numbers of thermal fatigue cycles, while thermal fatigue cracks in the matrix would permit oxidation of the reinforcement.

Elastic Shear Stresses

In order to evaluate equation (15) for shear stress, it is necessary to determine the appropriate values of K where

$$K = \frac{(\sigma_\theta + \sigma_R)}{\sigma_x} \tag{17}$$

By referring to figures 17 and 18, it is possible to select corresponding values of σ_θ,

σ_R, and σ_x for given values of V_r and to determine values of K for $V_r \leq 0.65$. For $V_r > 0.65$, K = 2 because of the assumption of hydrostatic stress. Values of peak shear stress in the matrix of the model fiber-reinforced composite are shown in figure 21. The maximum values occur at a fiber fraction of approximately 0.80 both on heating and cooling. This maximum is about 135 ksi (935 MN/m^2) on cooling and about 40 ksi (276 MN/m^2) on heating. It is apparent that the elastic shear stresses in the matrix are equal to or in excess of the estimated matrix shear strengths (60 ksi (413 MN/m^2) at 80^o F (26.5^o C) and 25 ksi (172 MN/m^2) at 2000^o F (1093.5^o C)) essentially over the practical range of fiber contents. The stresses for composites with a fiber content below about 23 percent will be conservative for reasons explained in appendix F.

Incidentally, because λ is greater for the fiber composite than for the laminate composite, the tip shear stresses in the fiber composite will decay more rapidly away from the tip than in the instance of the laminate composite.

All of the discussion pertaining to the effects of shear stress in laminate composites is, of course, germane to fiber-reinforced composites.

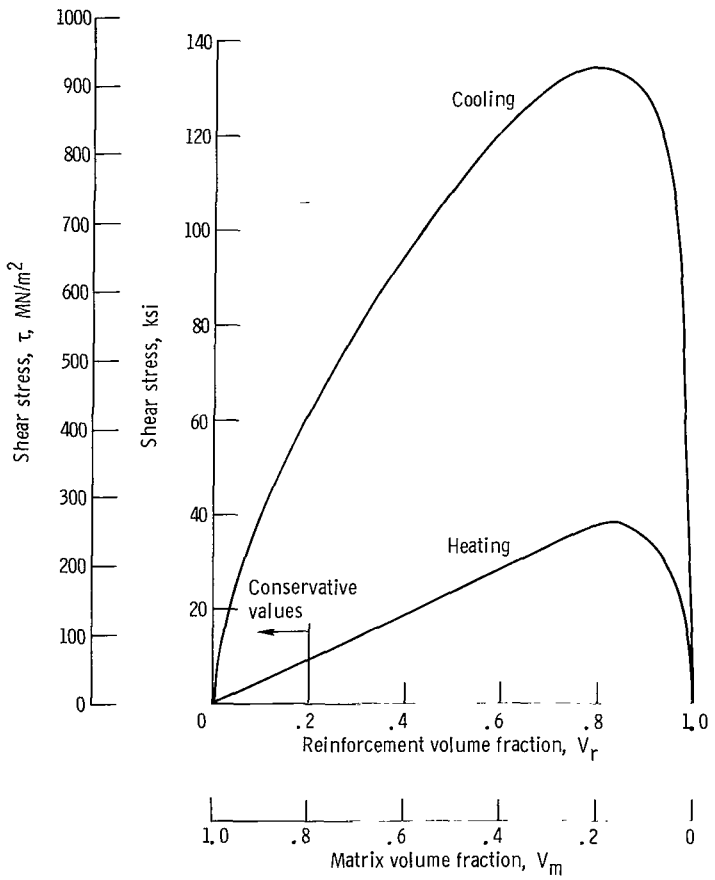

Figure 21. - Peak elastic shear stresses in tungsten-fiber-reinforced - 80Ni+20Cr-matrix composite. After heating or cooling between 80° and 2000° F (26.5° and 1093.5° C).

EXPERIMENTAL STUDIES OF FIBER-REINFORCED COMPOSITES

A study of limited scope was run on fiber-reinforced metallic-matrix composites to determine whether the fiber-reinforced composites could be damaged by heat-cool cycles; that is, to determine whether cyclic variations of temperature, which an actual fiber-reinforced composite might be exposed to, would produce microstructural evidence of composite damage. As before, the concern was with possible gross effects that might become evident in a limited number of cycles rather than a concern with relatively large numbers of cycles that might be required to produce thermal fatigue.

Materials, Apparatus, and Procedure

Two specimens of tungsten fiber-reinforced copper were evaluated; one specimen contained about 0.40 volume fraction tungsten and the other contained about 0.70 volume fraction tungsten. These particular composites were used because they were available from a previous study conducted at this laboratory and because they were felt to be metallurgically sound specimens. Further, the coefficient of thermal expansion of copper approximates that of nickel base alloys; the copper is presumably quite ductile and is theoretically nonreactive with tungsten. The last two characteristics would suggest that this system would tend to minimize any possible cyclic effects. The fiber was nominally 0.005 inch (0.0125 cm) in diameter. The composites were made by an infiltration technique such as described in reference 19. The specimens were initially about 1-inch (2.5-cm) long by 1/3 inch (0.13 cm) in diameter. The 0.40-volume-fraction tungsten composite had macroporosity. The 0.70-volume-fraction tungsten composite appeared free of macroscopic porosity. A small disk was taken from each of the two composite specimens. The larger portion of each composite was polished on either end to aid in subsequent examinations. Each disk was metallographically polished on one of its surfaces.

Each of the larger specimens was placed into a metallic foil heat-treating envelope along with a small amount of aluminum oxide (Al_2O_3) powder to prevent adherence of the specimen to the envelope. Each envelope was folded and then inserted into second envelopes. A thermocouple was inserted between the envelopes of one of the specimens to monitor temperature. The specimens were inserted simultaneously into an air atmosphere furnace which had been preheated to 1600° F (877° C). This temperature was purposely chosen to keep the test temperature well below the melting point of the copper matrix. The total time in the furnace for each heating cycle was 20 minutes, of which time 18 minutes were required for the thermocouple to reach 1600° F (877° C). The specimens, still in their protective envelopes, were cooled to ambient temperature;

they were removed from the furnace and placed on refractory brick. A temperature of 180° F (76° C) was indicated after 20 minutes of cooling. The heat-cool cycles was applied to each specimen six times. The external surfaces of these specimens were then examined macroscopically. In addition, about one-third the length of each specimen was subsequently mounted longitudinally and polished for metallographic study and for additional heat-cool study in a hot-stage microscope.

The specimens of 0.40- and of 0.70-volume-fraction tungsten fiber which were studied in a hot-stage microscope were heated from ambient temperature to 1652° F (900° C) and back to ambient. The time to heat was about 50 seconds and the time to cool was about 10 seconds. The dwell time at temperature was from 5 minutes to as long as 2 hours, and the number of heat-cool cycles was from 1 to 18 cycles. These specimens were photographed while in the hot-stage microscope. Film speeds of 1 to 20 frames per second were used. The intent of these particular studies was to determine whether damage could be initiated in the specimens by heat-cool cycles and to follow the damage in the first cycle, and in some cases in succeeding cycles, by means of a photographic record.

Initial studies which were for the primary purpose of developing methods, were performed on the transverse (disk) specimens. Subsequent studies were performed on longitudinal specimens. The longitudinal specimens were obtained from the 1/3-inch (0.13-cm) lengths which were in turn obtained from the original specimens following six heat-cool cycles in the air atmosphere furnace. The 1/3-inch (0.13-cm) long specimens which had been mounted, were removed from their mounts and cut into longitudinal specimens. The longitudinal specimens were cut to about 0.25 inch (0.625 cm) long so they would fit into the hot-stage microscope. The transverse and the longitudinal specimens were examined using conventional microscopy before and after hot-stage microscopy, in order to observe their entire cross sections before and after heating. The area under view in the hot-stage microscope was a small portion of the total surface area.

Results and Discussion

After the six heat-cool cycles in the air atmosphere furnace, each of the two fiber composite specimens sustained macroscopic change or damage. The tungsten fibers, which had been flush in both the specimens, were found now to extend beyond the matrix, at either end of either specimen. The tungsten fibers also protruded slightly beyond the peripheral confines of the matrix in the case of the 0.70-volume-fraction composite. The total length, as well as the diameter, was essentially unchanged in both instances. The protrusion was more pronounced at one edge of each specimen, and it was generally more pronounced at both edges for the 0.40-volume-fraction tungsten specimen. The edge protrudence of the fibers is shown in figure 22. Further, the 0.40-volume-

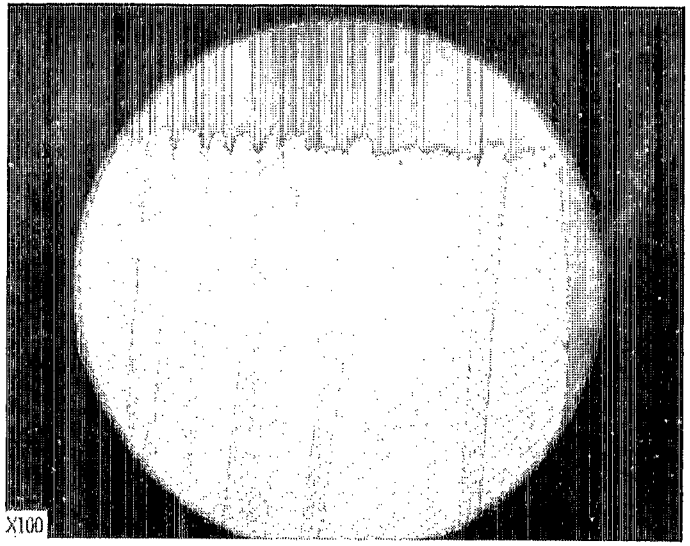

(a) Fiber volume fraction, 0.40. Note relative contraction of matrix.

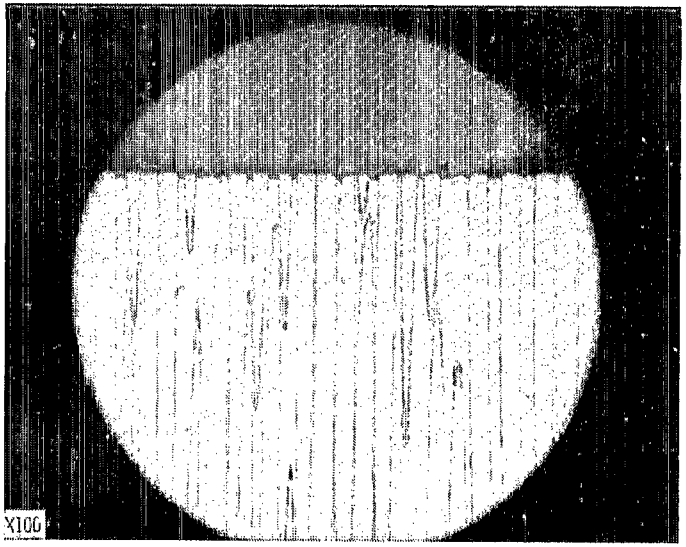

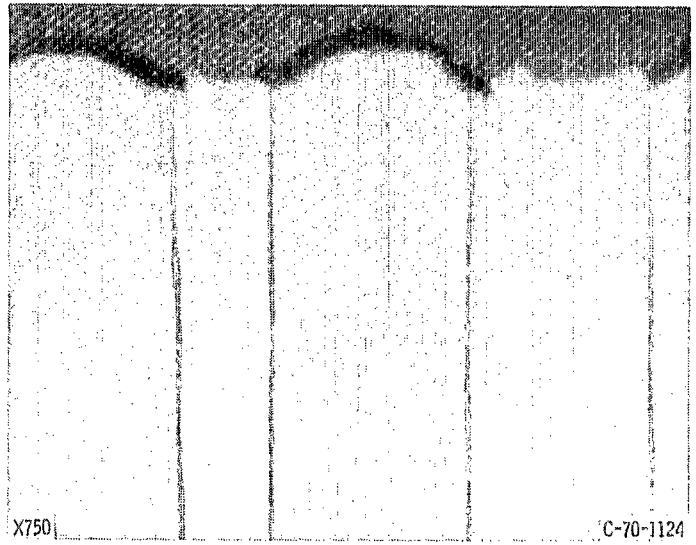

(b) Fiber volume fraction, 0.70.

Figure 22. - Tungsten-fiber - copper-matrix after 6 heat-cool cycles to 1652° F (900° C) in air furnace. Photographs reduced by 20% in reproduction.

fraction tungsten-fiber composite had an external crack about half-way along its length. The crack was partially circumferential and partly longitudinal (fig. 23).

The protrusion of the tungsten fibers beyond the confines of the matrix may have been the result of one or more possible factors, but, because of uncertainties and questionable relevancy, this was not pursued.

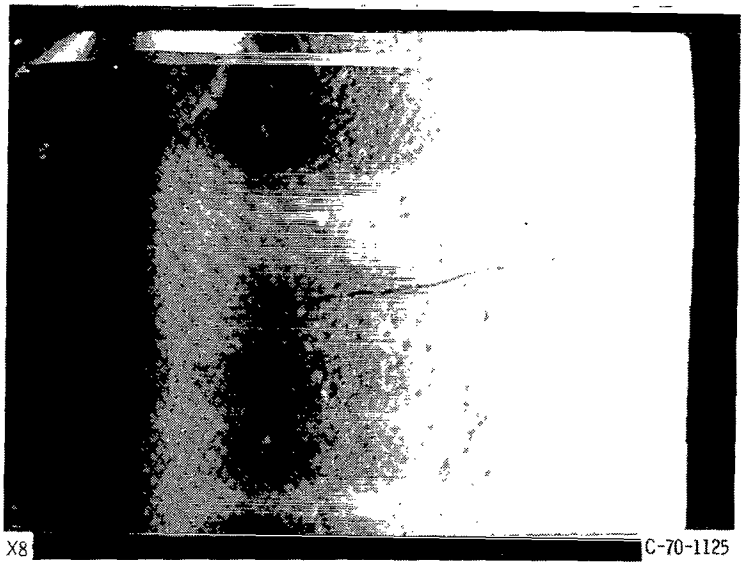

Figure 23. - Tungsten-fiber composite after six heat-cool cycles to and from 1600° F (877° C) in air furnace. Fiber volume fraction, 0.40. Note external crack.

The peripheral crack in the matrix of the 0.40-volume-fraction tungsten-fiber composite is attributed to a nonuniform distribution of fibers which allowed the generation of sufficiently high tensile stresses in the copper on cooling to cause fracture.

Microexamination of the 0.70-volume-fraction tungsten specimen indicated microfracturing of the matrix after the six heat-cool cycles (fig. 24). There was no indication of microcracks in the instance of the 0.40-volume-fraction tungsten-fiber-reinforced composite. The microfracturing in the 0.70-volume-fraction tungsten specimen could have occurred either while cooling or heating.

Exposure of a longitudinal section of a 0.70-volume-fraction tungsten fiber-reinforced composite to 1652° F (900° C) for 5 minutes in the hot-stage microscope resulted in deformation in the matrix, leading to eventual fracturing of the matrix. The deformation and subsequent fracturing occurred after the specimen had been at temperature for about 2 minutes. The specimen is shown before and after fracture in figure 25. The application of an additional 18 cycles resulted in a few more cracks and the accentuation of existent cracks. Also, matrix recrystallization occurred. This is shown in the post-test photomicrograph of figure 26.

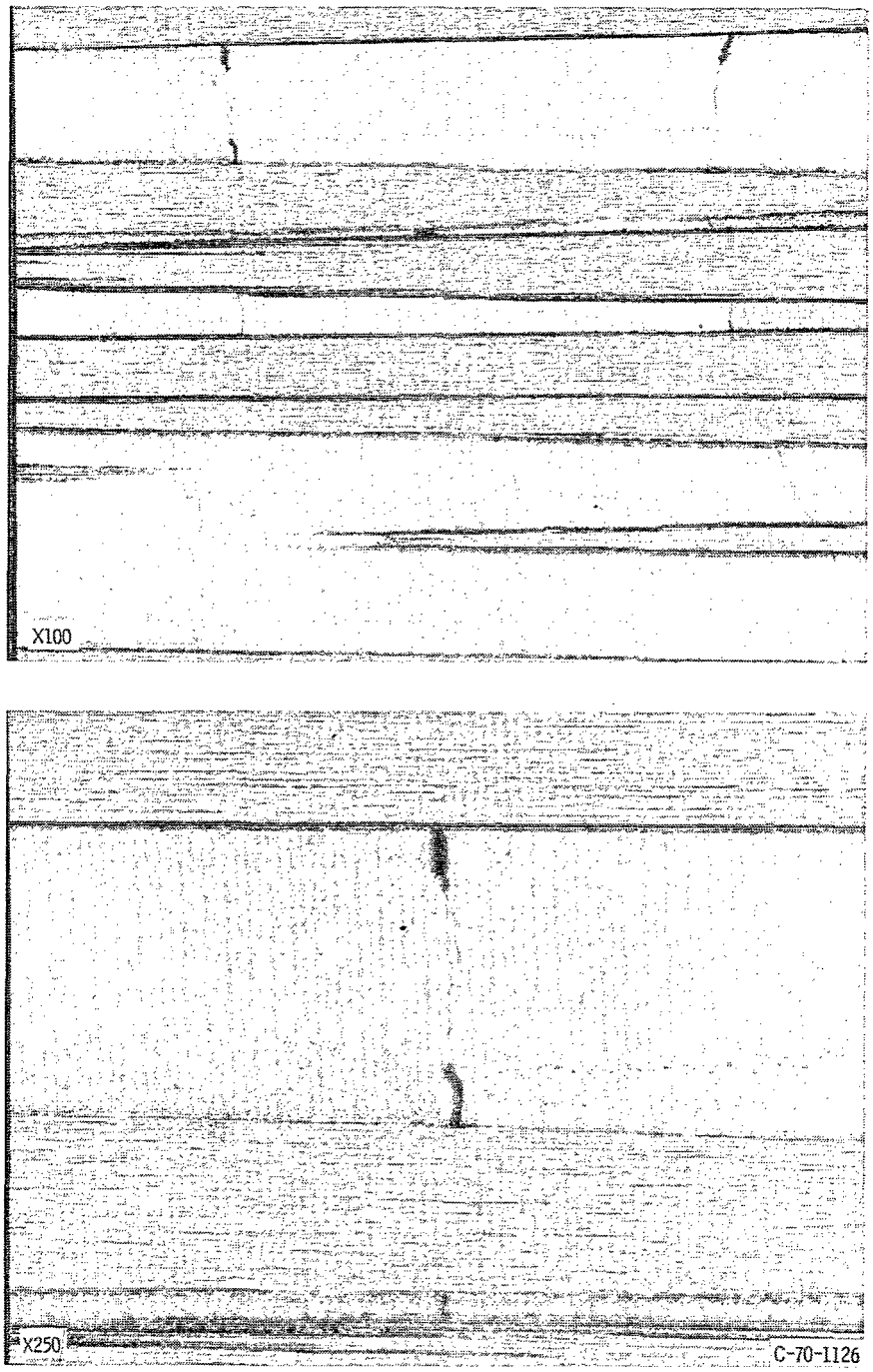

Figure 24. - Tungsten-fiber composite after six heat-cool cycles. Fiber volume fraction, 0.70. Specimens were chemically polished, Note matrix cracks.

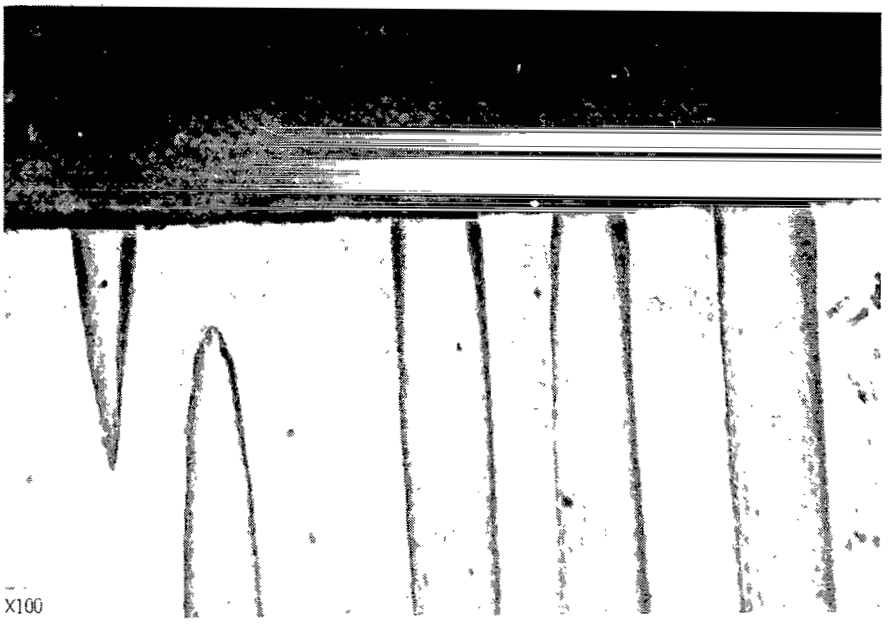

(a) Before heating.

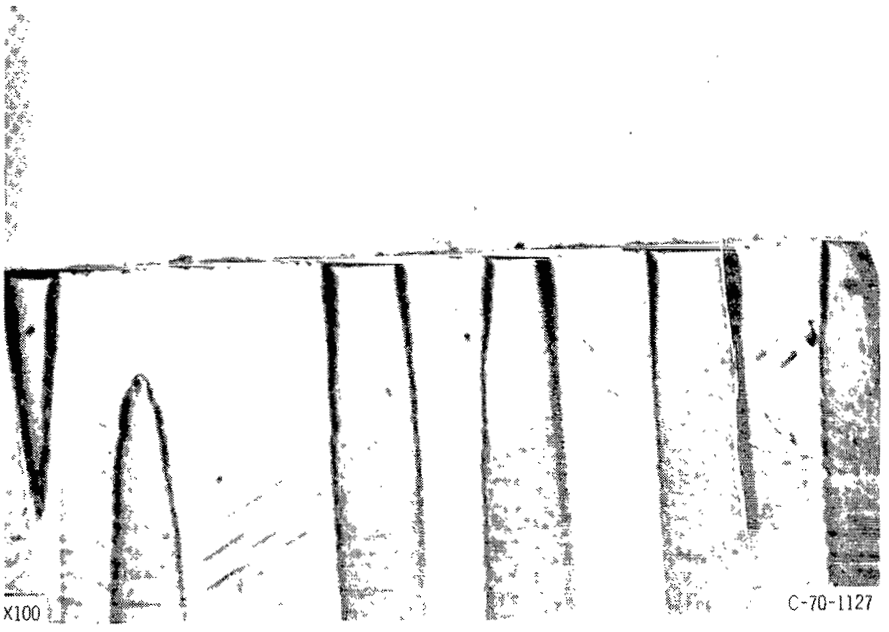

(b) After heating. Note matrix fractures and strains.

Figure 25. - Tungsten-fiber composite before and after one heat cycle to 1652 F (900 C) in hot-stage microscope. Fiber volume fraction, 0.70.

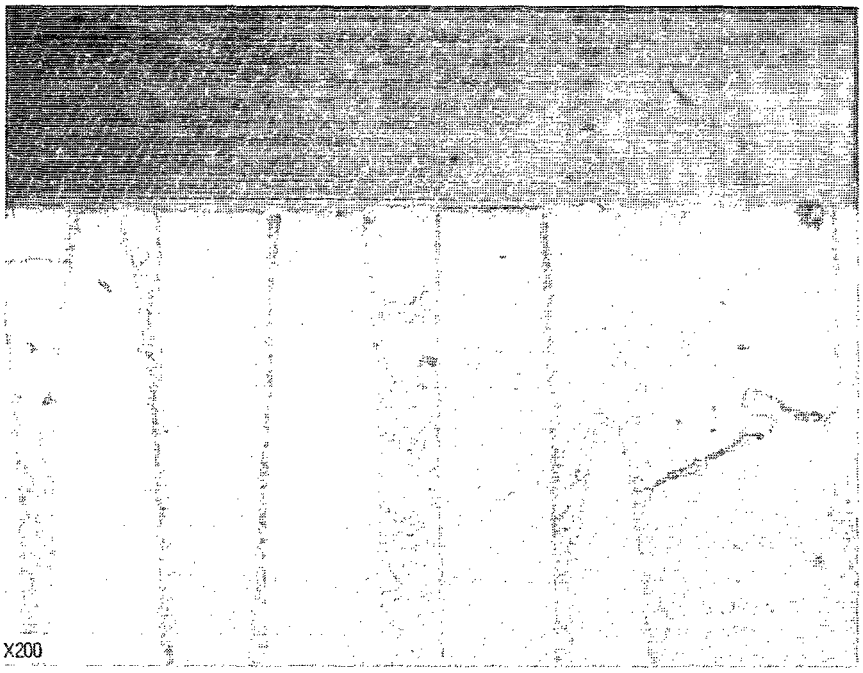

(a) Strain fracture and recrystallization in matrix.

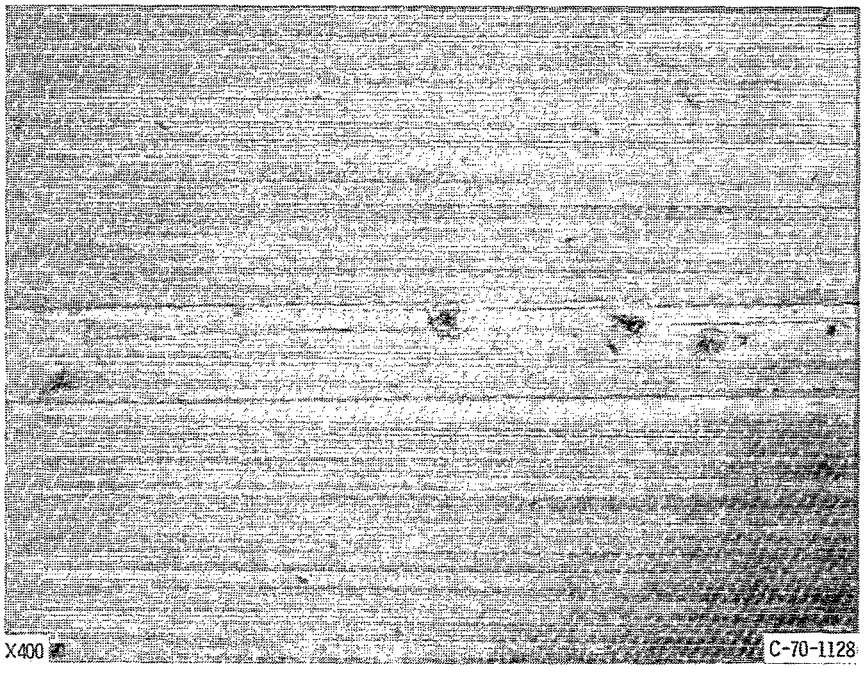

(b) Longitudinal cracks in matrix.

Figure 26. - Tungsten-fiber composite after 18 cycles of heating to and cooling from 1652° F (900° C) in hot-stage microscope. Fiber volume fraction, 0.70. (Photographed outside hot-stage microscope.)

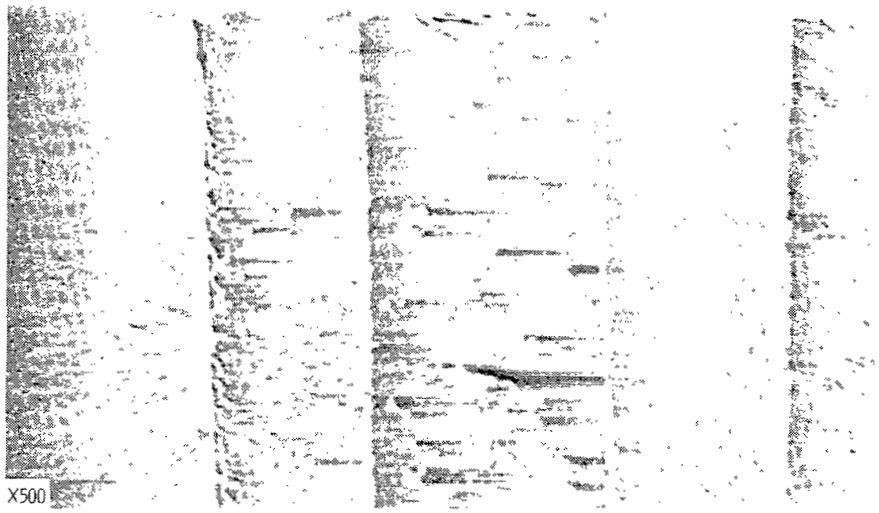

(a) Before heating.

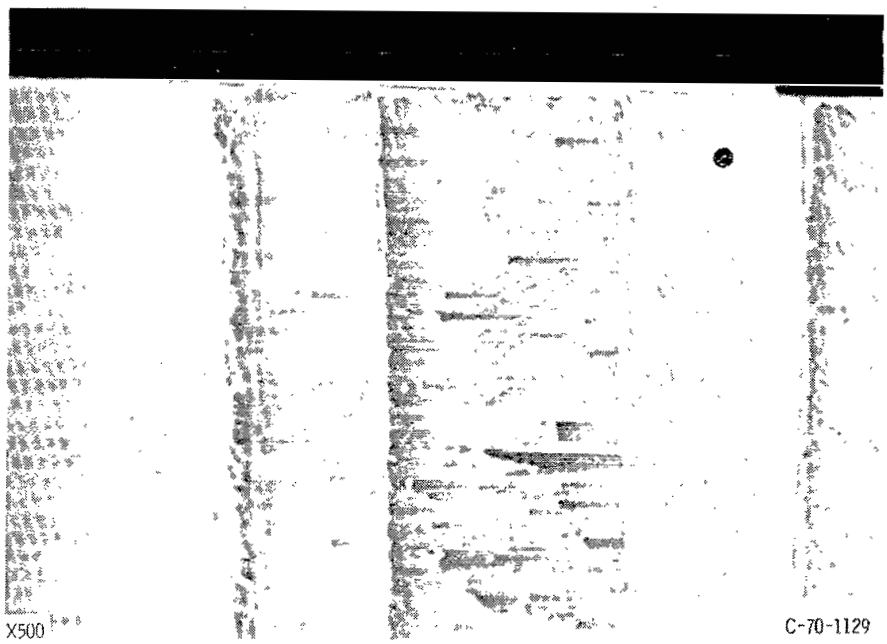

(b) After heating. Note strain lines in matrix.

Figure 27. - Tungsten-fiber composite before and after one heat-cool cycle to 1652 F (900 C) in hot-stage microscope. Fiber volume fraction, 0.40. (These photomicrographs were made from a positive, hence the detail is reversed from previous figure 25.)

Although the matrix of the 0.70-volume-fraction tungsten composite appeared to have sustained damage from the previous six heat-cool cycles in the air atmosphere furnace and although there was indication of residual matrix porosity (or microdamage from the previous six heat-cool cycles), it is evident that the heating cycles in the hot-stage microscope produced additional matrix damage. The matrix damage, which occurred while at temperature, could have resulted from radial tensile, tangential compressive, or shear stresses developed in the matrix upon heating.

A 0.40-volume-fraction tungsten specimen was given 14 heat-cool cycles in the hot-stage microscope. Matrix deformation was observed on the first cycle during heating (fig. 27). The deformation became more pronounced with each cycle until matrix recrystallization, which occurred at about the 10th cycle, obscured any further effects.

The calculated elastic stresses that would be generated in a composite with tungsten fibers circumscribed by a copper matrix are presented in table VIII. These values are approximate for the case where a fair number of fibers are at the surface and do not have a circular cross-section.

In order to assess the significance of the stress values in table VIII, it is necessary

TABLE VIII. - CALCULATED ELASTIC STRESSES IN TUNGSTEN-FIBER-REINFORCED - COPPER-MATRIX COMPOSITES

(a) Cooling from 1650° to 80° F (1093.5° to 26.5° C)

Reinforcement volume fraction	Constituent	Tensile or compressive stress							
		σ_θ		σ_R		σ_x		$\tau_{\theta x}$	
		ksi	MN/m^2	ksi	MN/m^2	ksi	MN/m^2	ksi	MN/m^2
0.40	Fiber	-71.4	-492	-71.4	-492	-292	-2020	-----	----
	Matrix	171	118	-71.4	-492	195	1350	148	1030
0.70	Fiber	-139	-956	-139	-956	-139	-956	-----	----
	Matrix	324	2240	324	2240	324	2240	80	551

(b) Heating from 80° to 1650° F (26.5° to 1093.5° C)

Reinforcement volume fraction	Constituent	Tensile or compressive stress							
		σ_θ		σ_R		σ_x		$\tau_{\theta x}$	
		ksi	MN/m^2	ksi	MN/m^2	ksi	MN/m^2	ksi	MN/m^2
0.40	Fiber	11.3	78	11.3	78	52.5	362	-----	----
	Matrix	-48.4	-334	11.3	78	-42.5	-294	71.1	490
0.70	Fiber	79.6	550	79.6	550	79.6	550	-----	----
	Matrix	-186	-129	-186	-129	-186	-129	66	455

to know the strengths of the matrix and reinforcement of the composite studied. These values are as follows:

Material	Temperature		Stress			
			σ_{ult}		b_τ	
(a)	°F	°C	ksi	MN/m^2	ksi	MN/m^2
Copper	80	26.5	19.3	133	9.5	60.9
	1650	900	1.5	10.4	.75	5.2
Tungsten	80	26.5	350	2410	----	----
	1650	900	75	518	----	----

[a]Copper data based on ref. 20; tungsten data based on ref. 10.

[b]$\tau \approx 1/2\ \sigma_{ult}$.

Referring now to table VIII, it is seen that the matrix tensile strengths and, in all probability, the matrix compressive and shear strengths can be exceeded in both the 0.40- and the 0.70-volume fraction composites upon either cooling or heating if there is no yielding. The fiber tensile strength could be exceeded in the 0.70-volume fraction tungsten composite during heating. The stress values in table VIII are based on elastic behavior and might not be reached because of plastic deformation. One would have to make a qualitative judgement and say that in the 0.40-volume-fraction tungsten composite, matrix fracture or deformation could occur either during heating or cooling. Most likely however, matrix yielding would occur at least during the initial cycling thus averting fracture or unbonding. Fiber damage might possibly occur in the 0.70-volume-fraction tungsten composite during heating, and matrix damage should occur during cooling. During heating, the matrix is assumed to be under hydrostatic compressive stress in the interior of the composite, but it is not under hydrostatic stress at the surface. This may be why the matrix appeared to have fractured while being heated in the hot-stage microscope; the matrix area viewed was at the surface. The matrix surface area viewed was not under hydrostatic stress and was free to experience strain (see fig. 24); the compressive stresses evidently were great enough to cause fracture.

The calculated stresses along with the assumption of plastic yielding in low volume-fraction composites are consistent with the observed results in that they suggest matrix yielding in the 0.40-volume-fraction tungsten-fiber composite and fiber or matrix fracture in the 0.70-volume-fraction tungsten fiber composite.

The results of the experimental study of the effects of heat-cool cycles on tungsten fiber-reinforced copper-matrix composites has shown that merely by heating and cooling,

structural changes can be introduced into them. Heating appeared to be more deleterious than cooling, but this may have been due to the particular specimen configuration used in the hot-stage microscope studies. Thermal gradients may have been introduced into these specimens and therefore could have been a contributing factor. But this is not considered too likely because of the high thermal conductivity of the copper matrix. One can tentatively conclude that high volume-fraction fiber-reinforced composites may sustain microstructural damage after a few heat-cool cycles or perhaps just as the result of cooldown after fabrication. Low volume-fraction fiber-reinforced composites appear more able to withstand heat-cool cycles but may ultimately experience thermal fatigue because of plastic strains.

SIGNIFICANCE OF MATHEMATICAL ANALYSIS AND EXPERIMENTAL RESULTS

Equations for calculating elastic stress and elastic-plastic stresses and strains were derived. Calculations of elastic stress were made for a model tungsten-fiber 80Ni+20Cr matrix composite. Estimates were also made of the maximum elastic-plastic stresses and strains that might occur in the model composite.

The stresses and strains in either constituent was a function of the relative amount of that constituent and the calculated elastic stresses could exceed the uniaxial tensile strength (and estimated matrix shear strength) of the constituents. By assuming the occurrence of elastic-plastic stresses and strains, rather than elastic behavior, actual stresses would be expected to be reduced compared with calculated elastic values and, in the case of the matrix, would be reduced to values approximating its yield strength. However, the reduction of elastic stresses by plastic strain can result in significant amounts of total strain and pose a possible thermal fatigue problem if the composite is thermally cycled.

Experimental studies on 0.40- and 0.70-volume-fraction tungsten fiber-reinforced - copper-matrix composites tended to confirm the mathematics. The studies indicated that it was possible to generate stresses that were great enough to fracture the matrix of the 0.70-volume-fraction tungsten-fiber composite, presumably upon heating in a vacuum to 1652° F (900° C). The stresses in a low volume-percent fiber-reinforced composite (i.e., 0.40-vol. fraction) which was heated to 1652° F (900° C), caused pronounced deformation of the matrix. Thus, high volume-fraction fiber composites ($0.65 < V_r < 0.90$) might be prone to fracture of the matrix in a few heat-cool cycles, but lower volume-percent fiber reinforced composites may experience matrix thermal fatigue after many cycles. However, very low volume-fraction reinforcement composites may be prone to reinforcement damage.

CONCLUDING REMARKS

Mathematical analyses, sample calculations, and limited experimentation all have indicated that thermal stress, arising from differences in the coefficients of thermal expansion of the constituents, can cause structural damage to laminated and fiber-reinforced composites when subjected to a thermal transition or to heat-cool cycles. It has been postulated throughout that damage is possible as a result of thermally induced stresses, and this is felt to have been borne out experimentally; if stress relief can occur by plastic flow, preventing immediate structural damage or damage in but a few cycles, then, under use-conditions involving a multiplicity of heat-cool cycles, thermal fatigue could result. The occurrence of thermal fatigue has not been necessarily borne out, however, Although this study strongly suggests the existence of a significant problem area, there is still very much that has to be understood regarding the susceptibility of metallic composite materials to structural and strength damage resulting from thermally induced stresses or strains due to differing coefficients of thermal expansion. Specific composite materials combinations may well possess adequate ductility to prevent the generation of critically high stresses and simultaneously possess ample thermal fatigue strength for heat-cool cycling applications. Additional study, both analytical and experimental, appears necessary.

The problem considered in this study, if of practical significance, might be minimized by a number of expedients suggested by the mathematics and experimental results; these include

(1) The obvious close matching of thermal expansivities
(2) Use of materials combinations with good interface bond strengths
(3) Use of relative amounts of constituents to minimize deleterious effects in the crucial constituent, that is, to reduce the stress in the critical constituent by increasing its volume fraction
(4) Use of appropriate spacings (or volume fractions) to reduce shear stress
(5) Use of intermediate zones of material with intermediate thermal expansivities
(6) Use of materials with good thermal fatigue properties

SUMMARY OF RESULTS AND CONCLUSIONS

An analytical and experimental study has been conducted to obtain indications of the possible effects of differences in coefficients of thermal expansion of the constituents on the structural integrity of laminate and fiber-reinforced composites. The study was made with reference to metallic systems, specifically to refractory-metal-reinforced superalloy-matrix composites. The results and conclusions of this heurestically oriented study are as follows:

1. Approximate equations were derived to permit the calculation of elastic stresses

in both laminate and fiber composites containing constituents with different coefficients of thermal expansion. The equations were applied to model laminate and fiber composites of tungsten-reinforcement and 80 nickel + 20 chromium matrix. Extremely high elastic stresses far in excess of the actual or estimated strengths of the constituents were calculated for temperature transitions between 80° to 2000° F (26.5° to 1093.5° C).

2. Approximate elastic-plastic solutions indicated that lesser stresses would occur as a result of plastic flow of either constituent. However, relatively substantial amounts of strain could be associated with these reduced stresses.

3. It is postulated that in heat-cool usage, large elastic stresses, sufficient to cause fracturing of either constituent or the interface, could quickly occur, on the one hand, but, if relieved by plastic deformation, could cause cycle limiting thermal fatigue, on the other hand.

4. Limited experimental studies on laminated tungsten-reinforced - 80 nickel + 20 chromium matrix composites containing about 50 volume percent of either constituent resulted in the following. With a slow heat-cool cycle (to and from 80° and 2000° F (26.5° and 1093.5° C)), 11 such cycles could cause extensive delamination in a specimen with 0.020-inch (0.050-cm) tungsten laminae and could cause fracture of the laminae in a specimen with 0.005-inch (0.0125-cm) tungsten laminae. With a rapid heat-cool cycle (to and from 80° and 1600° F (26.5° and 877° C)) a specimen with 0.020-inch (0.05-cm) tungsten laminae could be debonded in one cycle. A specimen with 0.005-inch (0.0125-cm) tungsten laminae could be severely damaged in three such cycles. And a specimen with 0.001-inch (0.0025-cm) tungsten laminae could evidence incipient damage after six such cycles.

6. Limited experimentation on fiber-reinforced composites indicated that microcracks could be induced in the matrix of a 0.70-volume-fraction tungsten-fiber - copper-matrix composite by a single heating to 1652° F (900° C) in a hot-stage microscope. A single heating to 1652° F (900° C) of a 0.40-volume-fraction tungsten composite in the hot-stage microscope produced pronounced matrix deformation. Heating was moderately rapid in both instances and may have contributed to the observed effects. Additional heat-cool cycles produced some additional fracturing in the 0.70-volume-fraction tungsten composite and a little more pronounced deformation in the 0.40-volume-fraction tungsten composite. Recrystallization of the copper matrix eventually occurred if heat-cool cycles were continued. Prior to the hot-stage microscope studies, these specimens were given six heat-cool cycles to 1600° F (877° C) and the 0.70-volume-fraction tungsten composite suffered matrix microcracking.

Lewis Research Center,
National Aeronautics and Space Administration,
Cleveland, Ohio, April 14, 1970,
129-03.

APPENDIX A

TENSILE AND COMPRESSIVE STRESSES IN LAMINATE COMPOSITES

The assumptions made for this analysis have already been enumerated on page 5. The mechanism by which tensile or compressive stresses are generated have already been discussed on page 6. In essence, the resultant strains in either the x or y direction (fig. 1) must be compatible and this may be expressed by the following equation:

$$\alpha_m \Delta T + \frac{(\sigma_x - \nu\sigma_y)_m}{E_m} + \epsilon_{mxp} = \alpha_r \Delta T + \frac{(\sigma_x - \nu\sigma_y)_r}{E_m} + \epsilon_{rxp} \tag{A1}$$

But, since $\sigma_x = \sigma_y$ (assumption (4), p. 5), equation (A1) can be expressed as

$$\alpha_m \Delta T + \frac{\sigma_{xm}(1 - \nu)_m}{E_m} + \epsilon_{mxp} = \alpha_r \Delta T + \frac{\sigma_{xr}(1 - \nu)_r}{E_r} + \epsilon_{rxp} \tag{A2}$$

A second condition that has to be fulfilled is that the total tensile force in the matrix be balanced by the total compressive force in the reinforcement and this is expressed by

$$P_m + P_r = 0 \tag{A3}$$

However, the composite consists of $N + 1$ laminae of matrix material, each of which sustains a tensile stress of σ_m, and N laminae of reinforcing material, each of which sustains a compressive stress of σ_r. Equation (A3) can then be expressed as

$$\frac{(N + 1)t_m\sigma_{mx}}{A_c} + \frac{NWt_r\sigma_{rx}}{A_c} = \frac{A_m}{A_c}\sigma_{mx} + \frac{A_r}{A_c}\sigma_{rx} = V_m\sigma_{mx} + V_r\sigma_{rx} = 0 \tag{A4}$$

Next, stresses and strains in a complex stress field can be expressed as effective or equivalent values by use of the generally accepted Von Mises' relation

$$\sigma_e = \frac{1}{\sqrt{2}}\left[(\sigma_x - \sigma_y)^2 + (\sigma_y - \sigma_z)^2 + (\sigma_z - \sigma_x)^2\right]^{1/2} \tag{A5}$$

from which it follows in this instance that

$$\sigma_e = \sigma_x = \sigma_y \tag{A6}$$

The strain in the plastic range may be taken as

$$\epsilon_{ep} = \frac{\sqrt{2}}{3}\left[\left(\epsilon_{xp} - \epsilon_{yp}\right)^2 + \left(\epsilon_{yp} - \epsilon_{zp}\right)^2 + \left(\epsilon_{zp} - \epsilon_{xp}\right)^2\right]^{1/2} \tag{A7}$$

Since

$$\sigma_x = \sigma_y$$

it follows that

$$\epsilon_{xp} = \epsilon_{yp}$$

Assuming incompressibility, it can be shown that

$$\epsilon_{zp} = -2\epsilon_{xp} \tag{A8}$$

Consequently, equation (A7) yields the relation

$$\epsilon_{xp} = \epsilon_{yp} = \frac{1}{2}\epsilon_{ep} \tag{A9}$$

By rearranging equation (A2) and substituting equations (A4), (A6), and (A9) into it, the following equations may be obtained:

$$\sigma_{em} = \frac{V_r E_r E_m}{(V_r E_r + V_m E_m)(1 - \nu)}\left[(\alpha_r - \alpha_m)\Delta T + \frac{1}{2}(\epsilon_{erp} - \epsilon_{emp})\right] \tag{A10}$$

$$\sigma_{er} = \frac{V_m E_r E_m}{(V_r E_r + V_m E_m)(1 - \nu)}\left[(\alpha_m - \alpha_r)\Delta T + \frac{1}{2}(\epsilon_{emp} - \epsilon_{erp})\right] \tag{A11}$$

Equations (A10) and (A11) can be used to calculate equivalent (or axial) stresses when elastic strains only occur in both the matrix and reinforcement or when either one or both of the components experience elastic-plastic strain. For the occurrence of elastic strains only, the plastic strain terms in equation (A10) and (A11) are omitted. Equivalent stress and strain have been used throughout to obtain indications of maximum strains.

Elastic-plastic solution. - For elastic-plastic solutions, however, equations (A10)

and (A11) must be solved by trial and error or by iteration using the stress-strain curves of the materials. This is relatively rapid when using computers. However, for the purpose of obtaining magnitudes, an expedient graphical method, although not necessarily rigorous, has been used in this report. The graphical method is based on the simultaneous satisfaction of two requirements: (1) the strains in the two constituents must be compatible and (2) the forces must be in equilibrium.

First, for compatibility of strain in the x (or y) direction the following condition must be fulfilled

$$\epsilon_{tmx} + \alpha_m \Delta T = \epsilon_{trx} + \alpha_r \Delta T \tag{A12}$$

However, for simplification it is assumed that all the strain is plastic. This assumption allows the use of Von Mises' equation for effective plastic strain, that is,

$$\epsilon_{ep} = \frac{\sqrt{2}}{3}\left[\left(\epsilon_{xp} - \epsilon_{yp}\right)^2 + \left(\epsilon_{yp} - \epsilon_{zp}\right)^2 + \left(\epsilon_{zp} - \epsilon_{xp}\right)^2\right]^{1/2}$$

Further, using the usual assumption of incompressibility, it can be determined that

$$\epsilon_{ep} = 2\epsilon_{xp} = 2\epsilon_{yp} \tag{A13}$$

Thus, using equations (A12) and (A13) and the assumption of complete plastic strain

$$\epsilon_{emp} - \epsilon_{erp} \approx 2(\alpha_r - \alpha_m)\Delta T \tag{A14}$$

Next, forces must be in equilibrium and satisfy the following equation

$$V_m \sigma_{em} + V_r \sigma_{er} = 0 \tag{A15}$$

Equations (A14) and (A15) can be solved using the appropriate stress-strain diagrams for the matrix and for the reinforcement. Corresponding values of σ_{em}, ϵ_{epm}, σ_{er}, and ϵ_{epr} can be obtained from these diagrams, which simultaneously satisfy equations (A14) and (A15). It should be noted that the values of σ and ϵ_p on any stress-strain diagram are assumed to correspond to values of σ_e and ϵ_{ep}. The values thus obtained will be estimates of the elastic-plastic stresses and strains and will be more accurate when the elastic strain is small compared with the plastic strain.

Another point to mention is that stress-strain diagrams for the temperature extremes (i.e., 80° F (26.5° C) or 2000° F (1093.5° C)) have been used, which assumes the absence of any stress relaxation.

APPENDIX B

ELASTIC SHEAR STRESSES IN LAMINATE COMPOSITES

The assumptions made have already been enumerated on page 7, as was the mechanism of stress generation. The region of interest is shown in figure 1, and the element of interest is located at $y = y_o$ and is near the tip of the composite (i.e., $x \approx 0$). A typical element is shown in figure 3(a).

The governing equation is derived from equilibrium of forces in the x direction. From figure 3(b),

$$\sum P = 0$$

or

$$\left(\sigma_{rx} + \frac{d\sigma_{rx}}{dx}\,dx\right)t_r W - \sigma_{rx} t_r W - 2W\tau_{mzx}\,dx = 0 \tag{B1}$$

From which it follows

$$t_r \frac{d\sigma_{rx}}{dx} - 2\tau_{mzx} = 0 \tag{B2}$$

The matrix is under pure shear as illustrated in figure 4. From the geometry of figure 4, the definition of shear strain, and Hooke's law, the following relations can be written, letting $\epsilon_{av}x$ equal the displacement at the tip of the composite

$$\gamma_{mzx} = \frac{2(u - \epsilon_{av}x)}{t_m} \tag{B3}$$

and

$$\tau_{mzx} = \gamma_{zx} G_m \tag{B4}$$

from which it follows

$$\tau_{mzx} = \frac{2G_m(u - \epsilon_{av}x)}{t_m} \tag{B5}$$

Also from Hooke's law

$$\sigma_{rx} = \frac{E_r}{1 - \nu_r^2} (\epsilon_{rx} + \nu_r \epsilon_{ry}) \tag{B6a}$$

and

$$\sigma_{ry} = \frac{E_r}{1 - \nu_r^2} (\epsilon_{ry} + \nu_r \epsilon_{rx}) \tag{B6b}$$

From the assumption that

$$\sigma_x = \sigma_y$$

it follows that

$$\epsilon_y = \epsilon_x$$

which, when substituted into (B6a), results in

$$\sigma_{rx} = \frac{E_r}{(1 - \nu_r)} \epsilon_x \tag{B7}$$

But since

$$\epsilon_x = \frac{du}{dx}$$

it follows that, for the reinforcement,

$$\sigma_{rx} = \frac{E_r}{(1 - \nu_r)} \frac{du}{dx} \tag{B8}$$

Using equations (B1), (B5), and (B8) and dividing by t_r results in

$$\frac{d^2u}{dx^2} - \frac{4G_m(1 - \nu)_r(u - \epsilon_{av}x)}{E_r t_r t_m} = 0$$

or

$$\frac{d^2u}{dx^2} - \frac{4G_m(1 - \nu)_r u}{E_r t_r t_m} = - \frac{4G(1 - \nu)_r \epsilon_{av} x}{E_r t_r t_m} \tag{B9}$$

Since equation (B9) is linear, it can be solved by superposition. For the homogeneous solution,

$$u_h = Ae^{-\lambda_1 x/t_m} + Be^{\lambda_1 x/t_m} \tag{B10}$$

where

$$\lambda_1^2 = \frac{4G_m(1 - \nu)_r t_m}{E_r t_r} \tag{B11}$$

The particular solution yields

$$u_p = \epsilon_{av} x \tag{B12}$$

and the solution now becomes

$$\left.\begin{aligned} u &= u_h + u_p \\ u &= \epsilon_{av} x + Ae^{-\lambda_1 x/t_m} + Be^{\lambda_1 x/t_m} \end{aligned}\right\} \tag{B13}$$

where λ_1 is given by equation (B11).

The boundary conditions for equation (B12) are as $x \to \infty$

$$\frac{d(u - \epsilon_{av} x)}{dx} \to 0$$

and at $x = 0$

$$\frac{E}{(1 - \nu)_r} \frac{du}{dx} = \sigma_{xr} = 0$$

Using these conditions yields

$$\frac{du}{dx} - \epsilon_{av} = 0 = 0 + \frac{dBe^{\lambda_1 x/t_m}}{dx} - B^{\lambda_1/t_m} e^{\lambda_1 x/t_m} \Bigg|^{x \to \infty}$$

hence

$$B = 0 \tag{B14}$$

Applying the second condition

$$\frac{du}{dx} = 0 = \epsilon_{av} - \frac{\lambda_1}{t_m} Ae^{-\lambda_1 x/t_m} \Bigg|^{x=0}$$

Hence

$$A = \frac{\epsilon_{av} t_m}{\lambda_1} \tag{B15}$$

and u now becomes

$$u = \epsilon_{av} x + \frac{t_m \epsilon_{av}}{\lambda_1} e^{-\lambda_1 x/t_m}$$

The shear stress is obtained by substitution of equation (B14) in equation (B5) yielding

$$\tau_{mzx} = \frac{2G_m}{t_m} \left(\frac{t_m \epsilon_{av} e^{-\lambda_1 x/t_m}}{\lambda_1} \right)$$

or

$$\tau_{mzx} = 2G_m \frac{\epsilon_{av} e^{-\lambda_1 x/t_m}}{\lambda_1} \tag{B16}$$

The average strain is obtained from the condition that at $x >> t_m$ (away from a tip),

$$\epsilon_{rx} = \frac{(1 - \nu)_r}{E_r} \sigma_{rx} + \alpha_r \Delta T \tag{B17a}$$

$$\epsilon_{mx} = \frac{(1 - \nu)_m}{E_m} \sigma_{mx} + \alpha_x \Delta T \tag{B17b}$$

It is also apparent that average stresses may be equated giving

$$\sigma_{mx} = \frac{t_r \sigma_{rx}}{t_m} \tag{B18}$$

Equating (B17a) and (B17b) and using equation (B18) yield the relation

$$\sigma_{rx}\left(\frac{1 - \nu_r}{E_r} + \frac{1 - N_m}{E_m} \frac{t_r}{t_m}\right) = (\alpha_m - \alpha_r)\Delta T$$

$$\sigma_{rx} = \frac{(\alpha_m - \alpha_r)\Delta T}{\frac{(1 - \nu_r)}{E_r} + \left(\frac{1 - \nu_m}{E_m}\right)\left(\frac{t_r}{t_m}\right)} \tag{B19}$$

and the average strain ϵ_{av}, becomes

$$\epsilon_{av,x} = \frac{(1 - \nu_r)}{E_r} \frac{(\alpha_m - \alpha_r)\Delta T}{\frac{(1 - \nu_r)}{E_r} + \left(\frac{1 - \nu_m}{E_m}\right)\left(\frac{t_r}{t_m}\right)}$$

or

$$\epsilon_{av,x} = \frac{(\alpha_m - \alpha_r)\Delta T}{1 + \left(\frac{1 - \nu_m}{1 - \nu_r}\right)\left(\frac{E_r}{E_m}\right)\left(\frac{t_r}{t_m}\right)} \tag{B20}$$

Using equation (B20) in equation (B16) yields the equation for shear stress at the interface or in the matrix at any point x

$$\tau_{mzx} = \left[\frac{(\alpha_m - \alpha_r)\Delta T}{1 + \left(\frac{1 - \nu_m}{1 - \nu_r}\right)\left(\frac{E_r}{E_m}\right)\left(\frac{t_r}{t_m}\right)} \right] \frac{2G_m}{\lambda_1} e^{-\lambda_1 x/t_m} \tag{B21}$$

where

$$\lambda_1^2 = \left[\frac{4G_m(1 - \nu_r)t_m}{E_r t_r} \right] \tag{B22}$$

The limitations of equation (B21) are discussed in appendix F.

APPENDIX C

TENSILE AND COMPRESSIVE STRESSES IN HIGH-VOLUME-FRACTION, FULL-LENGTH FIBER-REINFORCED COMPOSITES

The assumptions to be used in this derivation have already been enumerated on page 29. The mechanism by which stresses are generated have already been alluded to on page 29 and is essentially as follows. After cooling, the average strains at a distance away from the ends must be compatible (i.e., the total strain in the fiber must be equal to the total strain in the matrix. And the forces must be in equilibrium. There will be equilibrium radial, tangential, and longitudinal stresses in both matrix and reinforcement (i.e., σ_R, σ_θ, and σ_x). First, consider the longitudinal or x direction stresses. Since the strains in this direction must be the same for both fiber and matrix; that is, the change in length of the fiber must be equal to the change in length of the matrix, the following relation between strains may be written:

$$\alpha_m \Delta T + \frac{\left(\sigma_x - \nu\sigma_\theta - \nu\sigma_R\right)_m}{E_m} + \epsilon_{mxp} = \alpha_r \Delta T + \left(\sigma_x + \nu\sigma_\theta + \nu\sigma_R\right)_r + \epsilon_{rxp} \qquad \text{(C1)}$$

or from assumption (3) (p. 29)

$$\alpha_m \Delta T + \frac{\sigma_{mz}}{E_m}(1 - 2\nu) + \epsilon_{mzp} = \alpha_r \Delta T + \frac{\sigma_{rz}}{E_r}(1 - 2\nu) + \epsilon_{rzp} \qquad \text{(C2)}$$

Since there must be equilibrium of forces, the following condition must also be satisfied

$$P_m + P_r = 0 \qquad \text{(C3)}$$

Each fiber of area a_r is assumed to be interacting with an area of matrix a_m, and since there are N fibers, equation (C3) can be represented as

$$Na_r\sigma_r + Na_m\sigma_m = 0 \qquad \text{(C4)}$$

Dividing through by the area of the composite A_c, gives

$$\frac{Na_r\sigma_r}{A_c} + \frac{Na_m\sigma_m}{A_c} = 0 \qquad \text{(C5)}$$

However, since area fraction and volume fraction are equal, equation (C5) can be written as

$$V_r\sigma_r + V_m\sigma_m = 0 \tag{C6}$$

Since there can be no plastic deformation in a condition of hydrostatic stress, the terms for plastic deformation are zero in equation (C2). Equation (C2) can now be written as

$$\alpha_m \Delta T + \frac{\sigma_{mzx}}{E_m}(1 - 2\nu) = \alpha_r \Delta T + \frac{\sigma_{Rx}}{E_r}(1 - 2\nu) \tag{C7}$$

Equation (C6) can be substituted into equation (C7), and by algebraic rearrangement the following equation representing the longitudinal stress in the matrix of the composite can be obtained

$$\sigma_{xm} = \frac{V_r E_r E_m(\alpha_r - \alpha_m)\Delta T}{(V_r E_r + V_m E_m)(1 - 2\nu)} \tag{C8}$$

In a similar fashion the following equation representing the longitudinal stress in the reinforcement (fiber) can be obtained

$$\sigma_{xr} = \frac{V_m E_r E_m(\alpha_r - \alpha_m)\Delta T}{(V_r E_r + V_m E_m)(1 - 2\nu)} \tag{C9}$$

Since $\sigma_x = \sigma_\theta = \sigma_R$ has been assumed, equation (C8) can also be used to obtain the radial and tangential stresses in the matrix and equation (C9) can also be used to obtain the radial and tangential stresses in the reinforcing fiber. Obviously, equivalent stresses and strains will be zero, but not necessarily the principal stresses.

APPENDIX D

TENSILE AND COMPRESSIVE STRESSES IN LOW-VOLUME-FRACTION, FULL-LENGTH FIBER-REINFORCED COMPOSITES

The assumptions made for this analysis have already been enumerated on page 30 and, the mechanism whereby the stresses are generated has been discussed on page 30. The basic equations that will be used have been derived by Timoshenko (ref. 21), and are

$$\sigma_R = \frac{a^2 p_i - b^2 p_o}{b^2 - a^2} - \frac{(p_i - p_o)a^2 b^2}{r^2(b^2 - a^2)} \tag{D1}$$

$$\sigma_\theta = \frac{a^2 p_i - b^2 p_o}{b^2 - a^2} + \frac{(p_i - p_o)a^2 b^2}{r^2(b^2 - a^2)} \tag{D2}$$

$$\delta = \frac{bp}{E_1}\left(\frac{b^2 + c^2}{c^2 - b^2} + \nu_1\right) + \frac{bp}{E_2}\left(\frac{a^2 + b^2}{b^2 - a^2} - \nu_2\right) \tag{D3}$$

where a, b, and c are radii of the cylinders shown in figure 13(d), p_i and p_o are internal and external pressures, respectively, and δ is the difference between fiber diameter and matrix element inner diameter after heating or cooling (in the absence of any mutual restraint).

Equations (D1) and (D2) may be used to express the stress in the matrix in which case p_o is assumed to be zero and the inner and outer radii are taken as b and c, respectively. The resulting equations are

$$\sigma_{mR} = \frac{b^2 p_i}{(c^2 - b^2)} - \frac{p_i b^2 c^2}{r^2(c^2 - b^2)} = \frac{b^2 p_i}{(c^2 - b^2)}\left(1 - \frac{c^2}{r^2}\right) \tag{D4}$$

and

$$\sigma_{m\theta} = \frac{b^2 p_i}{(c^2 - b^2)}\left(1 + \frac{c^2}{r^2}\right) \tag{D5}$$

Now, if b and r, are divided by c to make the equations dimensionless, the following equations result:

$$\sigma_{mR} = \frac{\beta^2 p_i}{1 - \beta^2}\left(1 - \frac{1}{\rho^2}\right) \tag{D6}$$

$$\sigma_{m\theta} = \frac{\beta^2 p_i}{1 - \beta^2}\left(1 + \frac{1}{\rho^2}\right) \tag{D7}$$

where

$$\frac{b^2}{c^2} = \beta^2$$

and

$$\frac{r^2}{c^2} = \rho^2$$

Further, if r is made equal to b, the inner radius, the preceding equations then become

$$\sigma_{mR} = -p_i \tag{D8}$$

and

$$\sigma_{m\theta} = \frac{\beta^2 + 1}{1 - \beta^2} p_i \tag{D9}$$

and give the maximum stress which is at the fiber interface. Equations (C1) and (C2) may also be used to express the stresses in the fiber. In the case of the fiber, the inner radius a becomes zero and the internal pressure is zero. However, the fiber is under some external pressure p_o. In a manner analogous to that just used, dimensionless equations may be derived for the stresses in the fiber and these equations are

$$\sigma_{rR} = -p_o \tag{D10}$$

$$\sigma_{r\theta} = -p_o \tag{D11}$$

Equations (D8) and (D9) give the stress at the interface between the fiber and matrix, and equations (D10) and (D11) indicate constant stresses anywhere along the radius of the

reinforcing fiber. Heating will reverse the stress directions.

It is apparent that the external pressure p_o on the fiber must equal this internal pressure on the matrix; that is,

$$p_o = p_i = p \tag{D12}$$

The value of p can be obtained from equation (C3) by setting δ equal to the difference between the fiber outer radius and the matrix inner radius after heating or cooling; that is,

$$\delta = b(\alpha_m - \alpha_r)\Delta T$$

Further in the derivation of the equation for p, the fiber and matrix are assumed to have different elastic moduli but equal values of Poisson's ratio, and the equation for p may be made dimensionless by dividing c by b. The resultant equation is then

$$p = \frac{(\alpha_m - \alpha_r)\Delta T\, E_m E_r (1 - \beta^2)}{E_r\left[\beta^2(1 - \nu) + 1 + \nu)\right] + E_m(1 - \beta^2)(1 - \nu)} \tag{D13}$$

Equations (D8) to (D11) and (D13) can be used to calculate the elastic stress in the matrix and in the fibers in principal directions transverse to the length of the composite. The preceding equations will give conservative results since they are predicated on the assumption of no stress interaction between adjacent matrix cylinders. Actually, there are stress interactions, and the strain at the periphery of each matrix cylinder would approach zero because of them. Reevaluation of the constants in equations (D1) to (D3) with the assumption that strain equals zero at c might be a better assumption to make particularly when there is a considerable amount of fiber; hence, equations (D1) to (D3) are probably conservative.

The longitudinal stresses in the reinforcing fiber and in the matrix may be derived by assuming compatibility of strain and equilibrium of stress. Doing this results in the following equations:

$$\frac{1}{E_m}\left[\sigma_{mz} - \nu(\sigma_{m\theta} + \sigma_{mR})\right] + \alpha_m \Delta T = \frac{1}{E_r}\left[\sigma_{rz} - \nu(\sigma_{r\theta} + \sigma_{rR})\right] + \alpha_r \Delta T \tag{D14}$$

and

$$V_m\sigma_m + V_r\sigma_r = 0 \tag{D15}$$

Inspection of equations (D6) and (D7) indicate that for the matrix

$$\left(\sigma_\theta + \sigma_R\right)_m = \frac{-2\beta^2}{1 - \beta^2} \tag{D16}$$

Inspection of equations (D10) and (D11) indicate that for the fiber

$$\left(\sigma_\theta + \sigma_R\right)_r = -2p \tag{D17}$$

By substitution of equations (D15) to (D17) into equation (D14) and by algebraic rearrangement, the following equations may be derived:

$$\sigma_{mx} = \frac{V_r E_r E_m(\alpha_x - \alpha_{rm})\Delta T + V_r \nu p\left(\frac{2\beta^2}{1 - \beta^2} E_r + 2E_m\right)}{V_r E_r + V_m E_m} \tag{D18}$$

and

$$\sigma_{rx} = \frac{V_m E_r E_m(\alpha_{rm} - \alpha_x)\Delta T - V_m \nu p\left(\frac{2\beta^2}{1 - \beta^2} E_r + 2E_m\right)}{V_r E_r + V_m E_m} \tag{D19}$$

Equations (D18) and (D19) may be used to estimate the elastic stresses in the fiber and in the matrix.

Elastic-Plastic Stresses and Strains

Equations (D8) to (D11) and (D19) are predicated on the assumption of elastic deformation and contain no terms for plastic deformation. But they can be used, in conjunction with the strain invariance principle, to estimate elastic-plastic stresses and strains. The strain-invariance principle (ref. 12) asserts that, in thermal strain problems, the total strain, that is, the elastic plus plastic strain, can be estimated by assuming completely elastic behavior and then calculating the elastic strain associated with a calculated elastic stress, even though this stress be beyond the yield strength.

The previously mentioned equations will be used to calculate elastic stress values for the θ, R, and x directions. Using these calculated values along with the strain invariance principle, the total strain in each of these directions will be calculated for

fiber-reinforced composites with fiber fractions up to 0.65. Equivalent total strains will be calculated for a given set of principal strains using the relation for ϵ_{et} in equation (35) of reference 22, that is,

$$\epsilon_{et} = \frac{\sqrt{2}}{3}\left[\left(\epsilon_\theta - \epsilon_R\right)^2 + \left(\epsilon_R - \epsilon_z\right)^2 + \left(\epsilon_z - \epsilon_\theta\right)^2\right]^{1/2}$$

Having calculated ϵ_{et} for a given value of V_r (or V_m), the appropriate stress-strain diagram (fig. 7) will be used to obtain estimates of the corresponding values of ϵ_{ep} and σ_e. With the value of ϵ_{et} known, the following equation (i.e., eq. (5) of ref. 22)

$$\epsilon_{et} = \frac{2}{3}\frac{1+\nu}{E}\sigma_e + \epsilon_{ep} \tag{D20}$$

will be used along with the stress-strain diagrams to get corresponding values of ϵ_{et}, ϵ_{ep}, and σ_e. The values of ϵ_{ep} and σ_e correspond to ϵ_p and σ of the appropriate stress-strain diagram. Values of ϵ_{et}, ϵ_{ep}, and σ_e, which satisfy both equation (D20) and the appropriate stress-strain diagram, are first approximations of equivalent stresses and strains and will indicate the plastic strain as well as the total strain that has occurred and what the corresponding stress is.

Stress-strain diagrams for the limiting temperatures (80° F (265° C) and 2000° F (1093.5° C)) will be used. The diagrams are used on the assumption that no relaxation occurs during the temperature change.

APPENDIX E

ELASTIC SHEAR STRESS IN FULL-LENGTH FIBER-REINFORCED COMPOSITES

The assumptions to be used in this analysis as well as the mechanism which generates shear stress in the matrix have been discussed on page 27.

The strain in the longitudinal or x direction of the composite may be expressed as

$$\epsilon_{rx} = \frac{\sigma_{rx}}{E} - \frac{\nu_r}{E}(\sigma_R + \sigma_\theta) \tag{E1}$$

Referring now to equations (D13) and (D17), it may be seen that, for a given composite having a specific relative amount of reinforcement and exposed to a specific ΔT,

$$\left(\sigma_R + \sigma_\theta\right)_r = -2P \tag{E2}$$

Equation (D19) can also be evaluated for the same set of specific conditions as equation (E2), so that for a set of specific values

$$\left(\sigma_R + \sigma_\theta\right)_r = K\sigma_{xr} \tag{E3}$$

where

$$K = \frac{(\sigma_R + \sigma_\theta)(V_r E_r + V_m E_m)}{V_m E_r E_m(\alpha_m - \alpha_r)\Delta T - V_r \nu p\left[\left(\frac{2\beta^2}{1-\beta^2}\right) E_r + 2E_m\right]}$$

By placing equation (E3) into equation (E1), the following equation may be obtained

$$\epsilon_{rx} = \frac{\sigma_{rx}}{E}(1 - K\nu_r) \tag{E4}$$

or

$$\sigma_{rx} = \frac{E}{(1 - K\nu_r)}\epsilon_{rx} = \frac{E}{(1 - K\nu_r)}\frac{du}{dx} \tag{E5}$$

Figures 14 and 15 show that equilibrium of forces between the fiber and its associated cylinder of matrix may be written as

$$\frac{\pi D_r^2}{4}\left(\sigma_x + \frac{d\sigma_x}{dx}\,dx - \sigma_x\right) - \pi D_r \tau_{m\theta x} = 0 \tag{E6}$$

or

$$\frac{D_r}{4}\frac{d\sigma_x}{dx} - \tau_{m\theta x} = 0 \tag{E7}$$

The equation for shear stress in the matrix of the fiber-reinforced composite is determined, in an analogous manner to that used in appendix B, for the laminate matrix. Figure 4 can be used again except $1/2\ t_m$ is now $(D_m - D_r)/2$ and the shear stress is

$$\tau_{m\theta x} = \frac{G_m(u - \epsilon_{av}x)}{\frac{D_m - D_r}{2}} \tag{E8}$$

Substitution of (E8) in (E7) results in

$$\frac{D_r}{4}\frac{d\sigma_x}{dx} - \frac{2G_m(u - \epsilon_{av}x)}{D_m - D_f} = 0 \tag{E9}$$

Next, differentiating equation (E5) and substituting it into equation (E7) result in

$$\frac{D_r}{4}\frac{E_r}{(1 - \nu K)_r}\frac{d^2u}{dx^2} - \frac{2G_m(u - \epsilon_{av}x)}{D_m - D_r} = 0 \tag{E10}$$

or

$$\frac{d^2u}{dx^2} - \frac{8G_m(u - \epsilon_{av}x)\,(1 - K\nu_r)}{(D_m - D_r)D_rE_r} = 0 \tag{E11}$$

An alternate of equation (E11) is

$$\frac{d^2u}{dx^2} - \frac{8G_m(1 - \nu K)_r\nu}{(D_m - D_r)D_rE_r} = \frac{8G_m(1 - K\nu_r)\epsilon_{av}x}{(D_m - D_r)D_rE_r} \tag{E12}$$

Solving this equation as before results in

$$u = \epsilon_{av}x + Ae^{-\lambda_2 x/(D_m - D_r)} + Be^{\lambda_2 x/D_m - D_r} \tag{E13}$$

where

$$\lambda_2^2 = \frac{8G_m(1 - K\nu_r)(D_m - D_r)}{D_r} \tag{E14}$$

Applying the same limit conditions as previously allows evaluation of the constants and results in

$$u = \epsilon_{av}x + \frac{(D_m - D_r)\epsilon_{av}}{\lambda_2} e^{\lambda_2 x/(D_m - D_r)} \tag{E15}$$

Equation (E15) is substituted into equation (E8) resulting in

$$\tau_{m\theta x} = \frac{2G_m(D_m - D_r)\epsilon_{av}e^{-\lambda_2 x/(D_m - D_r)}}{(D_m - D_r)\lambda_2} \tag{E16}$$

or

$$\tau_{m\theta x} = \frac{2G_m\epsilon_{av}e^{-\lambda_2 x/(D_m - D_r)}}{\lambda_2} \tag{E17}$$

Since strains must be compatible, it follows that

$$\epsilon_{av,x} = (1 - \nu K_r)\frac{\sigma_{rx}}{E_r} + \alpha_r \Delta T = (1 - \nu K_m)\frac{\sigma_{mx}}{E_m} + \alpha_m \Delta T \tag{E18}$$

It also follows that

$$D_r^2\sigma_r + \left(D_m^2 - D_r^2\right)\sigma_m = 0 \tag{E19}$$

From which it follows that

$$\sigma_{mx} = \frac{D_r^2}{\left(D_m^2 - D_r^2\right)}\sigma_r \tag{E20}$$

Using the relations of equations (E18) and (E19), it follows that

$$\sigma_{rx}\left[\frac{(1 - K\nu_r)}{E_r} + \frac{(1 - K\nu_m)}{E_m}\frac{D_r^2}{\left(D_m^2 - D_r^2\right)}\right] = (\alpha_m - \alpha_r)\Delta T \tag{E21}$$

This equation may be arranged to give

$$\sigma_{rx} = \frac{(\alpha_m - \alpha_r)\Delta T}{\frac{(1 - K\nu_r)}{E_r} + \frac{(1 - K\nu_m)}{E_m}\frac{D_r^2}{\left(D_m^2 - D_r^2\right)}} \tag{E22}$$

or expressed in terms of strain

$$\epsilon_{av,x} = \frac{(\alpha_m - \alpha_r)\Delta T}{1 + \frac{(1 - K\nu_m)}{(1 - K\nu_r)}\left(\frac{E_r}{E_m}\right)\frac{D_r^2}{\left(D_m^2 - D_r^2\right)}} \tag{E23}$$

This equation may be substituted into equation (E17) to give the final equation which expresses the shear stress in the matrix of the fiber-reinforced composite

$$\tau_{m\theta x} = \frac{(\alpha_m - \alpha_r)\Delta T\, 2G_m e^{-\lambda_2 x/(D_m - D_r)}}{\left[1 + \frac{(1 - K\nu_m)}{(1 - K\nu_r)}\left(\frac{E_r}{E_m}\right)\frac{D_r^2}{\left(D_m^2 - D_r^2\right)}\right]\lambda_2} \tag{E24}$$

where

$$\lambda_2^2 = \frac{8G_m(1 - \nu K)_r(D_m - D_r)}{D_r} \tag{E25}$$

The relative breadth of matrix is subject to the limitations discussed in appendix F.

APPENDIX F

ASSUMPTION INHERENT IN SHEAR-STRESS ANALYSES

It is assumed that uniform shear will take place in the matrix as long as the matrix thickness does not exceed the reinforcement thickness in the case of laminate composites or as long as the interfiber spacing (i.e., matrix thickness) does not exceed the fiber diameter in the case of fiber reinforced composites.

The shear lag analysis then applies to laminate composites whose reinforcement volume fraction is greater than 0.5; that is, $V_r \geq 0.5$.

In the case of a fiber-reinforced composite with a hexagonal array of fibers (see sketch)

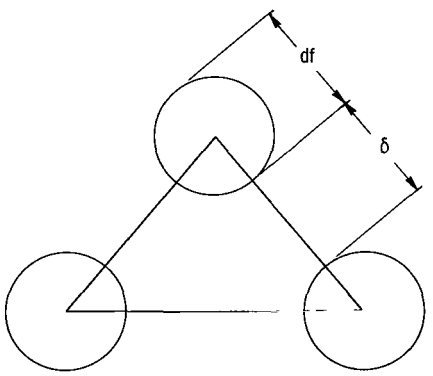

it can be determined that the ratio of fiber to matrix is

$$V_r = \frac{3x\frac{1}{6}\frac{\pi d_f^2}{4}}{\frac{1}{2}\left(d_f + \delta\right)^2 \frac{\sqrt{3}}{2}} \tag{F1}$$

Equation (F1) can be reduced to

$$V_r = \frac{\pi d_f^2}{2x\frac{4}{2}\left(2d_f\right)^2 \frac{\sqrt{3}}{2}} = \frac{\pi}{\sqrt{3}} \approx 0.23 \tag{F2}$$

when $\delta = d_f$.

Therefore, the shear lag analysis, under the assumptions made, is applicable to fiber-reinforced composites, with hexagonal arrays of fibers and with

$$V_r \geq 0.23$$

It can be readily shown that for square arrays of fibers

$$V_r \geq 0.19$$

As a generalization, the shear lag analysis is assumed valid for fiber-reinforced composites when the volume fraction of fiber is in excess of about 20 percent. With the exception perhaps of whisker-reinforced composites, most filament-reinforced composites will have a V_r greater than about 0.25 to 0.30; hence, the shear analysis is applicable for most practical fiber composites. In the case of laminates, it is conceivable that $V_r < 0.5$, in which case equations (B3) and (B2) are not necessarily applicable for the lower amounts of reinforcement.

The limitation of the shear lag analysis is assumed to be that the matrix thickness does not exceed the reinforcement thickness as illustrated in figure 28(a). If the matrix thickness exceeds the reinforcement thickness as shown in figure 28(b), it is then assumed that the shear deformation occurs in a region not exceeding $r/2$ in thickness. On this assumption the actual shear angle at the tip γ_3 (of fig. 28(b)) would be greater than the shear angle assumed by use of the shear lag analysis γ_2. Hence, the tip shear stresses associated with γ_3 would be greater than those associated with γ_2, and shear stresses based on a shear lag analysis would be lower bound values where $m > r$. The derived equations (B21) and (E24) will give lower boundary shear stress values for those cases where $V_r \gtrsim 0.5$ and $V_r \gtrsim 0.2$ for laminate and fiber composites, respectively. A more complex analysis such as that presented in reference 23, would be necessary to treat the problem of lower volume-fraction reinforced composites.

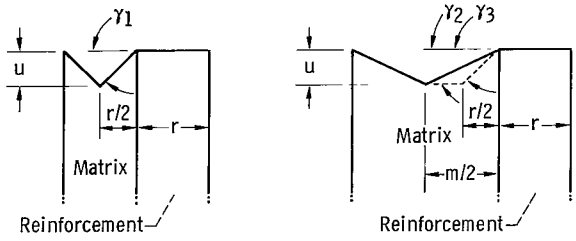

(a) Assumption made in shear lag analysis; that is, matrix spacing is equal to or less than reinforcement thickness or diameter and shear in the matrix extends for a distance r/2. Therefore, $\gamma_1 = 2u/r$.

(b) Matrix spacing greater than reinforcement thickness or diameter. When shear in the matrix occurs for a distance of r/2 rather than m/2, $\gamma_2 = (2u/m) < \gamma_3 = 2u/r$.

Figure 28. - Shear occuring in matrix whose thickness is (a) equal to or less than the thickness or diameter of the reinforcement or (b) greater than the thickness or diameter of the reinforcement.

REFERENCES

1. Dean, A. V.: The Reinforcement of Nickel-Base Alloys with High Strength Tungsten Wires. Rep. NGTE-R-266, National Gas Turbine Establishment, Apr. 1965.
2. Petrasek, Donald W.; Signorelli, Robert A.; and Weeton, John W.: Refractory Metal Fiber Nickel Alloy Composites for Use at High Temperatures. Presented at the 12th National Symposium, Society of Aerospace Material and Process Engineers, Anaheim, Calif., Oct. 10-12, 1967. (See also NASA TN D-4787, 1968).
3. Baskey, R. H.: Fiber-Reinforced Metallic Composite Materials. Clevite Corp. (AFML-TR-67-196, DDC No. AD-825364), Sept. 1967.
4. Lawley, Alan; Gaigher, Horace L.; and Schuster, Sidney: Deformation Characteristics of Thin Foils and Composites. Rep. F-A2366, Franklin Inst., Jan. 1964. (Available from DDC as AD-430902).
5. Covert, R. A.; and Rabinowicz, E.: An Investigation of Metallic Thin Film Composite Materials. Alloyd Electronics Corp. (ASD-TDR-62-617), June 1962.
6. Embury, J. D.; Petch, N. J.; Wraith, A. E.; and Wright, E. S.: The Fracture of Mild Steel Laminates. Trans. AIME, vol. 239, no. 1, Jan. 1967, pp. 114-118.
7. Scala, E.: Design and Performance of Fibers and Composites. Fiber Composite Materials. ASM, 1965, pp. 131-156.
8. Holliday, Leslie, ed.: Composite Materials. Elsevier Publ. Co., 1966, p. 125.
9. Greszczuk, L. B.; Miller, R. J.; and Netter, W. C.: Development of a System for Biaxial Prestressing Brittle Materials. Rep. DAC-62389, McDonnell-Douglas Corp. (NASA CR-98136), Sept. 1968.
10. Anon.: Tungsten - Bibliography 1953-1958. Physical Properties and Phase Diagrams. Sylvania Electric Products, Inc., 1959.
11. Gluck, Jeremy V.; and Freeman, James W.: Effect of Creep-Exposure on Mechanical Properties of 80Ni-20Cr and TZM Molybdenum Alloys. Michigan Univ. (ASD-TR-61-339), Sept. 1961.
12. Anon.: Technical Catalogue NcR-58, Driver Harris Co.
13. Weiss, V.; and Sessler, J. G., eds.: Aerospace Structural Metals Handbook. Vol. 2A. Syracuse Univ. Press, 1963.
14. Manson, S. S.: Thermal Stress and Low-Cycle Fatigue. McGraw-Hill Book Co., Inc., 1966.
15. Dorn, John E., ed.: Mechanical Behavior of Materials at Elevated Temperatures. McGraw-Hill Book Co., Inc., 1961.

16. Carden, A. E.: Thermal Fatigue of a Nickel-Base Alloy. Paper 64-MET-2, ASME, May 1964.

17. Johnston, James R.; Weeton, John W.; and Signorelli, Robert A.: Engine Operating Conditions that Cause Thermal-Fatigue Cracks in Turbojet-Engine Buckets. NASA Memo-4-7-59E, 1959.

18. Johnston, James R.; Freche, John C.; and Signorelli, Robert A.: Transient Temperature Profiles and Calculated Thermal Strains of Turbojet-Engine Buckets. NASA TN D-848, 1961.

19. McDanels, David L.; Jech, Robert W.; and Weeton, John W.: Stress-Strain Behavior of Tungsten-Fiber-Reinforced Copper Composites. NASA TN D-1881, 1963.

20. Petrasek, Donald W.: Elevated-Temperature Tensile Properties of Alloyed Tungsten Fiber Composites. NASA TN D-3073, 1965.

21. Timoshenko, Stephen: Advanced Theory and Problems. Part II of Strength of Materials. Third ed., D. Van Nostrand and Co., 1956.

22. Mendelson, A.; and Manson, S. S.: Practical Solution of Plastic Deformation Problems in the Elastic-Plastic Range. NASA TR R-28, 1959.

23. Haener, Juan; and Ashbaugh, Noel: Three-Dimensional Stress Distribution in a Unidirectional Composite. J. Composite Mat., vol. 1, no. 1, Jan. 1967, pp. 54-63.

NASA-Langley, 1970 —— 17 E-4768

NATIONAL AERONAUTICS AND SPACE ADMINISTRATION
WASHINGTON, D. C. 20546

OFFICIAL BUSINESS

FIRST CLASS MAIL

POSTAGE AND FEES PAID
NATIONAL AERONAUTICS AND
SPACE ADMINISTRATION

040 001 42 51 3DS 70212 00903
AIR FORCE WEAPONS LABORATORY /WLOL/
KIRTLAND AFB, NEW MEXICO 87117

ATT E. LOU BOWMAN, CHIEF, TECH. LIBRARY

POSTMASTER: If Undeliverable (Section 158 Postal Manual) Do Not Return

"The aeronautical and space activities of the United States shall be conducted so as to contribute . . . to the expansion of human knowledge of phenomena in the atmosphere and space. The Administration shall provide for the widest practicable and appropriate dissemination of information concerning its activities and the results thereof."

— NATIONAL AERONAUTICS AND SPACE ACT OF 1958

NASA SCIENTIFIC AND TECHNICAL PUBLICATIONS

TECHNICAL REPORTS: Scientific and technical information considered important, complete, and a lasting contribution to existing knowledge.

TECHNICAL NOTES: Information less broad in scope but nevertheless of importance as a contribution to existing knowledge.

TECHNICAL MEMORANDUMS: Information receiving limited distribution because of preliminary data, security classification, or other reasons.

CONTRACTOR REPORTS: Scientific and technical information generated under a NASA contract or grant and considered an important contribution to existing knowledge.

TECHNICAL TRANSLATIONS: Information published in a foreign language considered to merit NASA distribution in English.

SPECIAL PUBLICATIONS: Information derived from or of value to NASA activities. Publications include conference proceedings, monographs, data compilations, handbooks, sourcebooks, and special bibliographies.

TECHNOLOGY UTILIZATION PUBLICATIONS: Information on technology used by NASA that may be of particular interest in commercial and other non-aerospace applications. Publications include Tech Briefs, Technology Utilization Reports and Notes, and Technology Surveys.

Details on the availability of these publications may be obtained from:

SCIENTIFIC AND TECHNICAL INFORMATION DIVISION

NATIONAL AERONAUTICS AND SPACE ADMINISTRATION

Washington, D.C. 20546